



ALMA MATER STUDIORUM  
UNIVERSITÀ DI BOLOGNA

ARCHIVIO ISTITUZIONALE  
DELLA RICERCA

## Alma Mater Studiorum Università di Bologna Archivio istituzionale della ricerca

Economic and environmental benefits by improved process control strategies in HCl removal from waste-to-energy flue gas

This is the final peer-reviewed author's accepted manuscript (postprint) of the following publication:

*Published Version:*

Dal Pozzo A., Muratori G., Antonioni G., Cozzani V. (2021). Economic and environmental benefits by improved process control strategies in HCl removal from waste-to-energy flue gas. WASTE MANAGEMENT, 125, 303-315 [10.1016/j.wasman.2021.02.059].

*Availability:*

This version is available at: <https://hdl.handle.net/11585/821276> since: 2021-05-31

*Published:*

DOI: <http://doi.org/10.1016/j.wasman.2021.02.059>

*Terms of use:*

Some rights reserved. The terms and conditions for the reuse of this version of the manuscript are specified in the publishing policy. For all terms of use and more information see the publisher's website.

This item was downloaded from IRIS Università di Bologna (<https://cris.unibo.it/>).  
When citing, please refer to the published version.

(Article begins on next page)

Economic and environmental benefits by improved process control strategies in HCl removal from waste-to-energy flue gas

HIGHLIGHTS

*Alessandro Dal Pozzo, Giacomo Muratori, Giacomo Antonioni, Valerio Cozzani\**

LISES - Dipartimento di Ingegneria Civile, Chimica, Ambientale e dei Materiali, Alma Mater Studiorum - Università di Bologna, via Terracini n.28, 40131 Bologna, Italy

(\*)*corresponding author*, Tel. +39-051-2090240, Fax +39-051-2090247, e-mail: [valerio.cozzani@unibo.it](mailto:valerio.cozzani@unibo.it)

- A methodology was outlined to test control strategies in operating facilities
- A virtual console was used to reproduce system behaviour
- Environmental, Economic and Technical performance indicators were defined
- Improved control strategies result in higher Environmental and Economic performance
- Full-scale test-runs confirmed the effectiveness of alternative control strategies

1 Economic and environmental benefits by improved process control strategies in HCl removal  
2 from waste-to-energy flue gas

3

4 *Alessandro Dal Pozzo, Giacomo Muratori, Giacomo Antonioni, Valerio Cozzani\**

5 LISES - Dipartimento di Ingegneria Civile, Chimica, Ambientale e dei Materiali, Alma Mater  
6 Studiorum - Università di Bologna, via Terracini n.28, 40131 Bologna, Italy

7

8 (\*)*corresponding author*, Tel. +39-051-2090240, Fax +39-051-2090247, e-mail:  
9 valerio.cozzani@unibo.it

10

## 11 Abstract

12 The control of HCl emission in waste-to-energy (WtE) facilities is a challenging flue gas  
13 treatment problem: the release of HCl from waste combustion is highly variable in time and  
14 the HCl emission standards are typically far lower in WtE than in any other industry.  
15 Traditional process control approaches in dry HCl removal processes are generally based on  
16 feeding a large excess of solid reactants to the system, to ensure robustness and a wide safety  
17 margin in the compliance to environmental regulations. This results in the production of a  
18 high amount of unreacted sorbents, strongly increasing the generation of solid wastes that  
19 need to be disposed. In the present study, an approach was developed to allow the  
20 implementation of improved control strategies for dry HCl abatement systems in operating  
21 full-scale facilities. Its objective is the reduction of the reactant feed and the waste  
22 production, while still providing an adequate safety margin for emission compliance. The  
23 approach was based on the reproduction of the behaviour of the real system in a virtual  
24 console that allows the extensive testing of alternative control strategies, limiting the need of  
25 demanding test-runs at the real plant. A test case on an Italian WtE facility demonstrated the  
26 capability of a control logic tuned in the virtual console to achieve a 13% reduction in the  
27 consumption of reactants and generation of process residues, with unchanged HCl removal

28 efficiency. The results evidence the wide opportunities for optimisation of dry acid gas  
29 removal systems, in particular when multistage systems are implemented.

30 **Keywords:** waste-to-energy, HCl, process optimization, dry sorbent injection.

## 31 1 Introduction

32 In a modern waste management system, waste-to-energy (WtE) facilities have the role to  
33 divert from landfilling waste streams for which recycling is currently technically or  
34 economically unfeasible (Nizami et al., 2016) and enabling their thermal valorisation (Arena  
35 et al., 2015), thus facilitating the transition to a circular economy (Bagheri et al., 2020; Van  
36 Caneghem et al., 2019). Thanks to increasingly ambitious environmental regulations, the  
37 emission of several air pollutants related to WtE operation has been reduced more than  
38 tenfold in the last decades (Ardolino et al., 2020; Damgaard et al., 2010). However, in the  
39 current holistic approach to environmental protection, the reduction of impacts has to go  
40 beyond the minimisation of the emission of pollutants at the stack of the plant. Also indirect  
41 impacts, e.g. those associated to the consumption of reactants and the production of process  
42 residues in the flue gas treatment system of the plant (Dal Pozzo et al., 2017; Dong et al.,  
43 2020; Lausset et al., 2016), needs to be minimised.

44 Hydrogen chloride (HCl) is a typical pollutant in WtE flue gases, arising from the combustion  
45 of waste containing chlorine (Zhang et al., 2019). Chlorine is widely dispersed amongst organic  
46 and inorganic compounds present in several waste items (Gerassimidou et al., 2020; Yang et  
47 al., 2018). Among the different techniques available for HCl removal (Bal et al., 2019; Dal  
48 Pozzo et al., 2019; Ephraim et al., 2019; Kameda et al., 2020), dry sorbent injection (DSI) is  
49 one of the technologies more frequently implemented (Beylot et al., 2018; Dal Pozzo et al.,  
50 2018a). DSI consists in the in-duct addition of an alkaline powdered reactant (e.g. calcium

51 hydroxide or sodium bicarbonate), which neutralises acid pollutants as HCl via gas-solid  
52 reaction (Antonioni et al., 2016). DSI, adopted in either single or two-stage configurations (Dal  
53 Pozzo et al., 2016; De Greef et al., 2013), is considered among the best available techniques  
54 for flue gas treatment in WtE installations recommended by the European Union (Neuwahl et  
55 al., 2019).

56 The main environmental drawback of DSI systems is the high stoichiometric excess of reactant  
57 feed that is required to achieve high HCl removal efficiency (Vehlow, 2015). The resulting  
58 excess consumption of reactant leads to the generation of relevant streams of solid process  
59 residues in the fabric filters, where they are collected together with fly ashes and  
60 micropollutants. The presence of these other components in the collected process residues  
61 causes the stream to be considered as hazardous waste and to require its disposal in  
62 dedicated landfill sites (Dal Pozzo et al., 2018b; Kameda et al., 2020).

63 In addition, given that the composition of the waste burnt in the combustion chamber of a  
64 WtE plant varies widely over time, the resulting extreme variability of HCl concentration at  
65 the inlet of the flue gas treatment section (Dal Pozzo et al., 2020) is an inherent instability  
66 that limits the effectiveness of conventional control strategies in calibrating the reactant feed  
67 needed to maintain a constant concentration setpoint at the outlet. Thus, the prevailing trend  
68 in control strategies is to calibrate the process control parameters of the DSI system on the  
69 safe side, and even more so accept high excess feed rates of reactants to minimise the  
70 possible occurrence of overruns of HCl emission limits at stack.

71 A more accurate setting of the DSI control system could ensure not only a safe compliance of  
72 emission limits at stack, but also a reduction of the consumption of reactants and the  
73 generation of process residues. These in principle represent an undesired environmental

74 burden shift between different compartments (from air to soil/water) (Bogush et al., 2015;  
75 Margallo et al., 2015; Quina et al., 2018).

76 The problem of the optimisation of flue gas treatment control with reference either to the  
77 WtE context or to acid pollutants (HCl, SO<sub>2</sub>, HF) is scarcely addressed in scholarly literature.  
78 Ting et al. (2008) described the design of a PID control for acid gas removal via semi-dry  
79 scrubbing in a WtE plant, with parameter tuning performed during commissioning operation.  
80 Gassner et al. (2014) explored the use of data-driven modelling approaches to describe the  
81 non-stationary operational behaviour of a semi-dry flue gas desulfurization process. Cignitti  
82 et al. (2016) developed a simple first principle model to predict the dynamics of a semidry SO<sub>2</sub>  
83 absorber in desulfurization units of coal-fired power plants, while Guo et al. (2019) used a  
84 hybrid approach, blending first principles and neural network, to model and optimise a wet  
85 flue gas desulfurization unit. Yet, the focus of these recent studies has been mainly the  
86 theoretical development of enhanced dynamic models of the process, rather than their  
87 implementation in real control schemes. In particular, to the best of the authors' knowledge,  
88 no previous paper addresses the potential environmental and economic advantages in terms  
89 of reduced reactant consumption and related waste generation achievable with process  
90 control optimisation in WtE acid gas removal.

91 Furthermore, control optimisation in the WtE context is made complex by the fact that  
92 conventional direct tuning via extensive test runs during plant operation is generally  
93 incompatible with the need to comply with strict HCl emission limits in presence of a highly  
94 variable inlet load of HCl coming from waste combustion. In this regard, the set-up of data-  
95 driven simulations of the real system in a virtual environment, as more and more frequently  
96 performed in the manufacturing (Goodall et al., 2019) and process industry (Kockmann,  
97 2019), could drastically reduce the need of field tests. By this strategy, the screening and the

98 tuning of new control settings is carried out directly in a virtual set-up, thus limiting the  
99 number of in-field test runs only to those needed for the initial calibration of the simulation  
100 and for the final trial of the new control system.

101 The present study focuses on the development of an approach for the optimisation of process  
102 control in a typical DSI system for HCl removal based on a virtual environment. A dynamic  
103 simulation of the dry treatment system was built in a virtual console implemented using the  
104 Simulink software. A data-driven process model, calibrated with a specific set of test data,  
105 nested into a reproduction of the control system of the DSI unit, was thus obtained and  
106 validated. The virtual console was used to test and tune an alternative control strategy, with  
107 the objective to reduce the stoichiometric excess of reactant associated to HCl removal. The  
108 alternative control was then tested in full scale at the real plant, demonstrating the potential  
109 for significant environmental and economic benefits deriving from the reduction in reactant  
110 consumption and related process waste generation.

111

112 2 Reference system and test facility

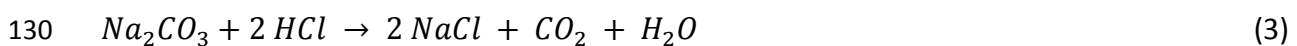
113

114 **2.1 HCl removal system**

115 The two-stage acid gas abatement system of a medium-sized (400 t/d of waste treated) WtE  
116 facility located in Northern Italy was used as case study. As shown in Fig. 1, this system is  
117 based on two consecutive steps of dry sorbent injection and filtration, taking place at ~180  
118 °C, downstream of the heat recovery section of the plant. In the first stage, calcium hydroxide,  
119  $\text{Ca(OH)}_2$ , is injected, triggering the following gas-solid reaction of HCl neutralisation (Iizuka et  
120 al., 2020):



122 A fabric filter separates the solid product of reaction from the flue gas, together with a  
123 relevant unreacted fraction of  $\text{Ca(OH)}_2$ , present both due to the excess feed of reactant and  
124 for the intrinsic diffusional limitations of gas-solid reaction (i.e. the phenomenon of  
125 incomplete conversion discussed by Antonioni et al., 2016). In the second stage, the dry  
126 injection is based on sodium bicarbonate,  $\text{NaHCO}_3$ . At the injection temperature and, in  
127 general, at  $T > 130$  °C (see Hartman et al., 2013),  $\text{NaHCO}_3$  decomposes to porous sodium  
128 carbonate ( $\text{Na}_2\text{CO}_3$ ), which in turn absorbs HCl (Dal Pozzo et al., 2019):



131 Again, the solid product of reaction and an unreacted fraction of reactant are collected by a  
132 fabric filter. This two-stage configuration is adopted in several European WtE installations and  
133 it is appreciated for its built-in redundancy in terms of emission control (De Greef et al., 2013)  
134 and its flexibility that allows different repartitions of abatement demand between the two  
135 stages (Dal Pozzo et al., 2016).



136 As shown in Fig. 1, the present study is focused on the optimisation of the control of the  
137  $\text{Ca(OH)}_2$  1<sup>st</sup> stage of acid gas removal, referred to in the following as dry sorbent injection (DSI)  
138 system. As discussed in the following, the optimisation and tuning of the process control of  
139 the 1<sup>st</sup> stage not only improves the performance of the stage, but, stabilising the HCl outlet  
140 concentration, it also favours the optimal performance of the 2<sup>nd</sup> stage.

141

## 142 **2.2 Process control**

143 In the test facility, a conventional process control scheme implemented in several similar  
144 plants is present. The operation of the two-stage acid gas abatement system is monitored by  
145 the continuous acquisition of flue gas composition data at the measurement points PM1, PM2  
146 and EM indicated in Fig. 1. The concentration of the main gas species at the sampling points,  
147 including the acid pollutants (HCl,  $\text{SO}_2$ , HF), is measured by Fourier-Transform infrared (FTIR)  
148 spectrometry, in compliance with CEN/TS 17337 (CEN, 2019), while the flue gas flowrate is  
149 determined at stack (point EM) by means of S-type Pitot tube velocity measurements.

150 In both the acid gas abatement stages, the distributed control system (DCS) of the plant  
151 controls the solid reactant feed based on the measured inlet and outlet mass flowrates of  
152 acid pollutants. A conditional logic selects the reactant feed rate as the maximum of two  
153 values, calculated as follows:

- 154 i. *Feedforward criterion.* The calculated feed rate is equal to the stoichiometric demand  
155 related to the abatement of the inlet mass flowrates of acid pollutants at PM1,  
156 increased by a 10% excess.
- 157 ii. *Feedback criterion.* The feed rate is calculated according to a Proportional Integral (PI)  
158 feedback formula based on the difference between a set-point for the outlet HCl  
159 concentration and the value measured at PM2.

160 The settings of the feedback control (proportional gain  $K_p = 5$  and integral gain  $\tau_I = 8$  s)  
161 provide an aggressive reaction, i.e. strong excess feed rates of reactant are delivered  
162 whenever the outlet HCl concentration exceeds the setpoint. Conversely, when the outlet HCl  
163 concentration is lower than the setpoint, the feed rate of reactant does not drop as  
164 significantly, because the feedforward criterion takes over. Thus, the combination of the  
165 feedforward and feedback criteria as detailed above realises an asymmetrical control action,  
166 in which the setpoint is actually treated as a threshold. The feedforward PI control works  
167 merely as an environmental safeguard, intended to act only if the feedforward is not capable  
168 to maintain the outlet below the given threshold. A survey carried out by the authors involving  
169 several Italian companies (HERAmbiente, HestAmbiente, IREN, Brianza Energia Ambiente)  
170 evidenced that this control strategy is typical of WtE acid gas abatement units, as the  
171 objective is to avoid any spike in outlet HCl resulting from a variation in the inlet HCl load  
172 coming from waste combustion (Muratori et al., 2020).

173

### 174 **2.3 Drawbacks of the reference control system**

175 The typical behaviour of the control system described in section 2.2 is shown in Fig. 2. Most  
176 of the time the control operates in feedforward mode and the feed rate of solid reactant is  
177 proportional to the inlet HCl load. However, when the outlet HCl flowrate exceeds its setpoint,  
178 the feedback mode takes over, imposing a relevant excess in feed rate to bring the HCl outlet  
179 back under the threshold as soon as possible. This behaviour determines a peak in reactant  
180 consumption but generates also unintended instability in the outlet HCl flow rate. As  
181 pinpointed by the arrows in Fig. 2, the spike of reactant feed manages to quickly reduce the  
182 outlet HCl flow rate, but such a reduction is often followed by a swift rebound of outlet HCl  
183 to high values that triggers another activation of the feedback control, resulting in another

184 spike of reactant feed. Since the layers of solid reactant accumulated over time on the fabric  
185 filter are known to play a major role in the overall acid gas removal action (Kim et al., 2017;  
186 Wu et al., 2004), the spikes of reactant feed might be detrimental because they induce  
187 unstable operation of the filter (Saleem and Krammer, 2012), activating frequent filter  
188 cleaning and reducing the residence time of reactant on the filter. The unstable HCl flow rate  
189 at the outlet of the 1<sup>st</sup> stage can in turn disturb the operation of the 2<sup>nd</sup> stage of acid gas  
190 removal.

191 In general, this control does not include the minimisation of reactant feed as a criterion and  
192 does not realise a rational use of reactant.

193

## 194 3 Methodology

### 195 3.1 Framework

196 Fig. 3 summarises the methodology developed to analyse the performance of alternative  
197 process control strategies for DSI, aimed at environmental and economic optimisation. The  
198 core element of the methodology is the development of a process simulation that allows  
199 exploring alternative control settings in a virtual console, while reducing the need for full-  
200 scale test-runs at the real plant. The process simulation duplicates into a software  
201 environment the process units and the control system of the actual facility. As sketched in Fig.  
202 3, building the simulation required: i) to reproduce the HCl removal process with a process  
203 model; and ii) to simulate the control structure of the DSI unit. The first task required the  
204 identification of an appropriate mathematical model for the description of the reaction  
205 process (see section 3.2) and its training and validation on plant data collected from test-runs

206 (see section 3.3). The second task was performed replicating the control architecture of the  
207 plant, briefly outlined in section 2.2, with a Simulink block diagram (see section 3.4).

208 The reliability of the simulation is validated considering the operating process control set-up  
209 in the real plant and comparing the outputs of the simulation with those recorded in the plant  
210 during normal operation, using the actual data as the input for the simulation. Once validated,  
211 the simulation can be used to screen and tune alternative control strategies, eventually  
212 leading to a new tuned control strategy that may be tested in the real plant, as in the test  
213 case that will be introduced in section 4.

214 Besides conventional indicators of process control performance, specific environmental and  
215 economic indicators (section 3.5) were defined to allow a comprehensive assessment of the  
216 performance of the alternative control strategies.

217

### 218 **3.2 Selection of data-driven process model and input variables**

219 As mentioned above, a mathematical model is required to reproduce the process dynamics  
220 in the simulation. The process model needs to predict how the instantaneous HCl removal  
221 efficiency varies depending on the inlet HCl concentration and the feed of solid reactant.

222 Given the intrinsic unsteady nature of the process, this task can be addressed only with a  
223 dynamic model capable of handling the rapidly changing operating conditions (e.g. variability  
224 of HCl concentration due to variability of waste composition). Existing simplified stationary  
225 models of acid gas removal that are typically applied for process optimisation studies  
226 (Harriott, 1990; Dal Pozzo et al., 2016) are clearly not apt for this task. On the other hand,  
227 phenomenological models (Antonioni et al., 2016; Foo et al., 2017; Montagnaro et al., 2016)  
228 that describe rigorously the kinetic and mass transfer phenomena involved in the gas-solid  
229 reaction process were typically derived from laboratory-scale data and are not suitable to

230 simulate full-scale systems, as stated by Gutiérrez Ortiz and Ollero (2008) and Gassner et al.  
231 (2014).

232 Therefore, a data-driven approach was chosen. A system identification procedure was  
233 performed to estimate the structure and the parameters of the model from observed input-  
234 output plant data (Ljung, 2010). A simple input-output polynomial model, *i.e.* the linear auto-  
235 regressive exogenous (ARX) model, was selected as base for the system identification. ARX  
236 models have already demonstrated to be reliable tools in emission control problems, e.g. in  
237 the prediction of NO<sub>x</sub> (Smrekar et al., 2013) or SO<sub>x</sub> (Choi et al., 2002) emissions from coal-  
238 fired boilers. They are appreciated for their transparency and ease of interpretation (Akinola  
239 et al., 2019). The general form of an ARX model is the following:

240

$$241 \quad y(t) = a_1 y(t-1) + \dots + a_{n_a} y(t-n_a) + \sum_i [b_{1,i} u_i(t-n_k) + \dots + b_{n_b,i} u_i(t-n_{k,i}-n_{b,i}+1)] + e(t) \quad (4)$$

242

243 where  $y$  is the output variable,  $u_i$  are the  $i$  input variables considered in the model, and  $e$  is  
244 the white-noise disturbance value. The values  $a$  and  $b$  are the model parameters, which can  
245 be represented in compact form in the parameter vector  $\theta$ :

246

$$247 \quad \theta = [a_1 \dots a_{n_a} \ b_{1,i} \dots b_{n_b,i}]' \quad (5)$$

248

249 This model structure implies that the output variable  $y$  at time  $t$  is predicted as a linear  
250 combination of past output values (autoregressive part of the model) and current and past  
251 values of the input variables (exogenous part of the model). The parameters  $n_a$  and  $n_{b,i}$  are,  
252 respectively, the number of past output samples and the number of past input samples (for  
253 each input variable  $i$ ) considered for the prediction of the current output. The model can also

254 consider input delay terms  $n_{k,i}$ , i.e. the number of input samples that occur before the input  
255 affects the output (also known as the dead time of the system). The use of past observations  
256 in the prediction of the output allows approximating also derivative terms by difference  
257 quotients, thus enabling the reproduction of the dynamics of the modelled system. The  
258 numbers  $n_a$ ,  $n_{b,i}$  and  $n_{k,i}$  are known as hyperparameters and represent the order of the model,  
259 *i.e.* they indicate the number of parameters to optimise in the training of the model.

260 For the sake of simplicity, a two-input single-output ARX model was chosen for the present  
261 study. The modelled output  $y$  is the HCl molar flowrate in the flue gas leaving the DSI system.  
262 The two input variables  $u_i$  are the inlet HCl molar flowrate and the molar flowrate of  $\text{Ca}(\text{OH})_2$   
263 fed to the DSI system.

264 In general, other variables might also affect the HCl removal process. The second most  
265 abundant acid compound in WtE flue gases,  $\text{SO}_2$ , can consume a fraction of the reactant feed  
266 (Zhang et al., 2019). Fluctuations in the flue gas flowrate can influence reactant residence  
267 time (Hunt and Sewell, 2015). Variations in the operating temperature of the HCl removal  
268 stage, e.g. caused by fouling in the heat recovery section upstream, can alter the gas-solid  
269 reaction kinetics (Dal Pozzo et al., 2018c). However, variations of temperature and flue gas  
270 flowrate are typically limited (see Fig. 2d and 2e) and, in the WtE plant under study, the inlet  
271  $\text{SO}_2$  concentration was a couple of orders of magnitude lower than that of HCl. Therefore,  
272 these variables were excluded in the formulation of the model.

273

### 274 **3.3 Calibration of the model**

275 As a data-driven model, the ARX structure requires a specific calibration on data from the  
276 actual DSI system modelled. Informative data can be obtained by open-loop tests, in which

277 the control of the system is deactivated and process performance is assessed by varying  
278 manually the feed rate of reactant while recording inlet and outlet HCl concentration.

279 The dataset  $Z^N$ , formed by N consecutive observations of the input and output variables,  
280 obtained from the tests has to be divided in: i) a training set  $Z_{trn}$ , used for the estimation of  
281 the optimal model parameters; and, ii) a cross-validation set  $Z_{crv}$ , used for the selection of the  
282 optimal order of the model.

283 A further validation data set,  $Z_{val}$ , obtained collecting operating data from the normal, closed-  
284 loop operation of the DSI system can be used for the assessment of the performance of the  
285 trained model.

286 Denoting as  $\hat{y}(t|\theta)$  the output prediction of the model, least-square method is used to  
287 estimate the parameter vector  $\theta^*$  that produces the best fit of the training data  $Z_{trn}$ :

$$288 \theta^* = \arg \min\{V(\theta, Z_{trn})\}, \quad \text{where } V(\theta, Z_{trn}) = \frac{1}{N_{trn}} \sum_{t=0}^{N_{trn}-1} (y(t) - \hat{y}(t|\theta))^2 \quad (6)$$

289 The cross-validation compares the performance of models with different orders, each with its  
290 optimal parameter vector  $\theta_i^*$ , estimated from the training set. The best model is the one for  
291 which  $V(\theta, Z_{crv})$  is the smallest. This procedure helps selecting a model structure without  
292 unnecessary complexity (*i.e.* order), as excessively complex models tend to overfit the training  
293 set and perform poorly in the cross-validation set. Lastly, the model with order and  
294 parameters optimised for the  $Z_{trn}$  and  $Z_{crv}$  sets can be tested on the validation set  $Z_{val}$  and the  
295 procedure can go on iteratively until a given threshold of performance is fulfilled.

296

### 297 **3.4 Virtual console**

298 The process model described in section 3.2 was integrated into a simulation environment,  
299 where also the control loop and the other components of the DSI system were cloned as in

300 the real plant. The virtual console simulating the operation of the real DSI system consists of  
301 four blocks, as shown in Figure 4.

302 The block “*Data import*” defines the inlet conditions of the simulation (inlet HCl concentration  
303 and flue gas flowrate). These may be either actual plant data, collected at the measurement  
304 point PM1 (see Fig. 1), or artificial data, created to test the system performance under specific  
305 strain.

306 The input data of the “*Data Import*” block are then transferred to the “*DTS*” and “*DCS*” blocks.

307 The “*DTS*” block contains the process model described in section 3.2. The “*DCS*” block  
308 simulates the control system described in section 2.2. Specifically, given as input signals the  
309 HCl load at the inlet of the DTS (provided by the “*Data Import*” block) and the HCl load at the  
310 outlet of the dry treatment system (modelled by the “*DTS*” block), this block evaluates with a  
311 clock time of 1 s the command input for the actuator that regulates the feed rate of Ca(OH)<sub>2</sub>.

312 The “*Actuator*” block simulates the operation of the screw feeder installed in the real plant.

313 The virtual actuator receives a percentage command of rotational speed calculated by the  
314 “*DCS*” block and transforms it into a molar feed rate of solid reactant to the “*DTS*” block,  
315 following a linear relationship between percentage command and feed rate that is  
316 characteristic of the real feeder. The response of the actuator was modelled as a first order  
317 transfer function:

318

$$319 \quad G(s) = \frac{R}{T_m \cdot s + 1} \quad (7)$$

320

321 where  $T_m$  is the actuation time of the screw feeder and  $R$  is the command to feed rate ratio.



322 This console allows the comparative testing of the behaviour of the DSI system under the  
323 default control (section 2.2) or an alternative control, as discussed in the test case described  
324 in section 4.

325

### 326 **3.5 Performance indicators selected to test alternative control strategies**

327 Both conventional indicators for process control performance and specific indicators  
328 capturing the environmental and economic performance of the process were defined to allow  
329 a comparison of alternative control strategies. The indicators are reported in Table 1  
330 alongside their values obtained for the test case that will be introduced in section 4.

331 With respect to conventional process control indicators, these address the stability of the  
332 output variables. The *instability of reactant injection*, expressed as the ratio of the CV of  
333 reactant injection to the CV of inlet HCl mass flow, measures the time variability of the feed  
334 rate of reactant imposed by the control system. All things equal, a control demanding less  
335 variable feed rates is preferred as it induces less mechanical stress on the feeding system. The  
336 *instability of HCl outlet*, expressed as the ratio of the CV of outlet HCl mass flow to the CV of  
337 inlet HCl mass flow, measures the variability of the HCl mass flow at the outlet of the DSI  
338 system.

339 Environmental indicators trace the material streams responsible for the indirect  
340 environmental burdens of HCl removal: the *specific consumption of reactant*, expressed as  
341 mass of reactant injected per mass of removed HCl, and the *specific generation of residues*,  
342 expressed as mass of process residues generated per mass of removed HCl. These indicators  
343 were monitored both for the Ca-based 1<sup>st</sup> stage and the bicarbonate-fed 2<sup>nd</sup> stage of HCl  
344 removal, as the stabilisation of control in the 1<sup>st</sup> stage (object of the study) can also result in  
345 a more stable operation for the 2<sup>nd</sup> stage. Therefore, an indicator of *overall generation of*

346 *residues*, encompassing both treatment stages, was also considered to have a complete  
347 picture of the environmental benefit of control optimisation.

348 Lastly, an indicator addressing *overall operating costs* was also estimated, by translating the  
349 streams of reactants and residues in operating costs considering their unit costs (see Table  
350 S1).

351

## 352 **4 Test Case**

353

### 354 **4.1 Definition of the test case**

355 The test facility described in section 2.1 was used to define a test case for the application of  
356 the methodology outlined in section 3. An open-loop test-run was used for the calibration of  
357 the ARX model, while the accuracy of the resulting virtual console in reproducing the system  
358 behaviour under its default control was assessed using several datasets available for the  
359 normal operation of the DSI system. An example of alternative control was proposed, tuned  
360 in the virtual console, then tested by full-scale test-runs on the real plant. The set of indicators  
361 defined in section 3.4 was adopted to quantify the improvements in the stability of process  
362 control and the economic and environmental performance.

363

### 364 **4.2 Calibration of the model and validation of the simulation for the test case**

365 The behaviour of the DSI system of the test facility was studied via step-response tests (Liu  
366 and Gao, 2012). Input excitations were applied to the system by varying stepwise the feed  
367 rate of  $\text{Ca(OH)}_2$ . The effect on system behaviour was recorded by continuous monitoring (30  
368 s resolution time) of the outlet HCl concentration (measurement point PM2 in Fig. 1), while  
369 the inlet HCl concentration was also recorded (measurement point PM1 in Fig. 1).

370 On the basis of the discussion provided in section 3.2, the ARX model was calibrated  
 371 considering the molar flowrate of inlet HCl (calculated from the measured inlet HCl  
 372 concentration and inlet flue gas flowrate) and the feed rate of Ca(OH)<sub>2</sub> as input variables,  
 373 while the molar flowrate of outlet HCl (product of the measured outlet HCl concentration  
 374 and outlet flue gas flowrate) is the modelled output.

375 The virtual console including the calibrated process model was then validated, comparing its  
 376 simulated outlet of HCl with the measured values in four datasets of operation of the DSI  
 377 system under the reference control, provided the same input data (see section 5.1). The  
 378 simulation error was quantitatively assessed by calculating a cumulative normalised root  
 379 mean squared error (RMSE):

$$380 \text{ Normalised RMSE } (t) = \frac{\sqrt{\frac{1}{n(t)} \sum_{i=1}^{n(t)} (y_i - \hat{y}_i)^2}}{\frac{\sum_{i=1}^{n(t)} y_i}{n(t)}} \quad (8)$$

381 where  $n(t)$  is the number of measurements/model evaluations at a given time.

382

### 383 4.3 Selection and tuning of an alternative control

384 Once the accuracy of the simulation results was demonstrated, the virtual console was used  
 385 to test alternative approaches to the control of HCl removal operation. In this test case, the  
 386 control logic described in section 2.2 (named in the following as “conventional control”) was  
 387 substituted with a simple feedback control (named in the following as “alternative control”).  
 388 Recalling Fig. 2, the conventional control is built to suppress any overrun of the setpoint of  
 389 outlet HCl concentration with a spike of Ca(OH)<sub>2</sub> feed. The consequences of such approach,  
 390 as illustrated in section 2.3, are an excess consumption of Ca(OH)<sub>2</sub> and unstable inlet  
 391 conditions for the 2<sup>nd</sup> HCl removal stage fed with NaHCO<sub>3</sub>, which, again, lead typically to an

392 excess consumption of  $\text{NaHCO}_3$ . Conversely, a properly tuned control in purely feedback  
393 action could limit the variability of both reactant feed and outlet HCl concentration.

394 The proposed feedback control is a simple proportional integral (PI) control. As the HCl inlet  
395 concentration signal is by nature highly variable and vulnerable to noise contamination  
396 (Coleman et al., 2019), the introduction of a derivative (D) control term was avoided, as it  
397 could generate system instability (Ting et al., 2008).

398 Hence, in the simulation the two parameters of the feedback control,  $K_p$  gain and  $\tau_I$  integral  
399 time, were tuned. The values of the optimised parameters were  $K_p = 2$  and  $\tau_I = 345$  s.

400

#### 401 **4.4 Performance assessment of the new control at the real plant**

402 Eventually, a comparative assessment of the performance of the conventional and alternative  
403 control was carried out at the test facility. The alternative control was easily implemented, by  
404 deactivating the feedforward control and updating the feedback settings to the tuned  
405 parameters.

406 The test consisted in comparing a period of DSI process operation with the alternative control  
407 with a period of operation with the conventional control. The HCl load released by waste  
408 combustion can vary widely over time, and any control logic would manage better a low and  
409 uniform inlet mass flow of HCl, rather than a high and fluctuating one. Thus, to ensure a  
410 proper comparison, a period of operation experiencing an almost equal inlet mass flow of HCl  
411 to that present during the test of the alternative control was selected as representative of the  
412 conventional control performance.

413 As a measure of variability of inlet HCl load, the coefficient of variation (CV) of the HCl mass  
414 flow during the test period was estimated:

415

416  $CV = \frac{\sigma}{\mu}$  (9)

417

418 where  $\sigma$  and  $\mu$  are respectively the standard deviation and the mean of the measurements of  
419 inlet HCl mass flow during the period of study. It was also ensured that the two periods of DSI  
420 operation used for the comparison exhibited a similar CV of HCl mass flow, as it will be  
421 discussed in section 5.3. The HCl removal efficiency  $X$  was also calculated as follows:

422  $X = \frac{\dot{m}_{HCl,in} - \dot{m}_{HCl,out}}{\dot{m}_{HCl,in}}$  (10)

423 The comparison among the performance of the alternative control strategies was carried out  
424 calculating the indicators discussed in section 3.5.

425

## 426 5 Results and Discussion

### 427 5.1 Results of the validation of the simulation

428 Figure 5 reports the performance of the virtual console in simulating the behaviour of the  
429 conventional process control of the DSI system on a sample dataset (other samples are shown  
430 in Figures S1-S3 in the Supporting Information, SI). The percentage command to reactant feed  
431 given by the real system and by the simulation are compared in Fig. 5a. Figure 5b compares  
432 the measured and the simulated outlet HCl mass flow. The yellow curve represents the set  
433 value of outlet HCl mass flow, which is a fluctuating value as it is defined as the product of the  
434 fixed setpoint of outlet HCl concentration (see e.g. Fig. 2b) and the variable value of the flue  
435 gas flowrate (see e.g. Fig. 2d). Again, it can be noticed that the conventional control treats the  
436 set value more like a threshold than a setpoint, as discussed in section 2.3. Figure 5c plots the  
437 cumulative average error of the simulation, represented as a normalised RMSE (introduced  
438 in section 4.2). The error increases over time, indicating a loss of performance of the process

439 model nested in the simulation, that is typical of error accumulation in models of  
440 autoregressive nature (Bazghaleh et al., 2013; Nelles, 2020). As evidenced also by the figures  
441 in the SI, the error grows faster when outlet HCl fluctuates widely, while it remains almost  
442 unchanged and may even decrease during periods of stable operation. It is clear that a simple  
443 ARX model, linear by nature, falls short of achieving an accurate instantaneous prediction of  
444 HCl outlet, which is the result of a complex and non-linear process involving gas-solid  
445 reactions both in duct and on filter bags. Nonetheless, the simulation captures the average  
446 system behaviour with acceptable resolution for the objective of the study.

447

## 448 **5.2 Results of the virtual testing of the alternative control**

449 The simulation was used for the tuning and for the virtual testing of the alternative PI control.  
450 The tuning of the alternative control by the methodology outlined in section 4.3 provided the  
451 following value for the control parameters: proportional gain  $K_p = 2$  and integral time  $\tau_I$  of  
452 345 s. It should be recalled that the PI settings of the feedback component of the conventional  
453 control (see section 2.2) are  $K_p = 5$  and  $\tau_I = 8$  s. The alternative control is less aggressive,  
454 with a reduced proportional action and a significantly higher integral time, which lowers the  
455 sensitivity of the control action to temporary deviations of the inlet HCl load. Figure 6a  
456 illustrates the different behaviour of the alternative control strategy compared to the  
457 conventional process control, on a data sample of 100 min. The simulation of the alternative  
458 control was started during a significant deviation of the measured HCl outlet concentration  
459 from the set-point value to emphasise the different mode of operation of the two control  
460 strategies. The feed rate variations imposed by the alternative control strategy are markedly  
461 smoother than those of the conventional control. The proposed strategy accepts momentary  
462 upticks in the HCl outlet concentration, whereas the action of the original control results in

463 spikes of reactant feed. Conversely, the alternative control strategy imposes a slightly higher  
464 feed rate than the original control during periods in which the latter operates in the  
465 feedforward mode. These opposite behaviours are evident from the plot of cumulated  
466 reactant consumption reported in Fig. 6c. Given that the variability of the reactant feed rate  
467 has been highlighted in section 2.3 as one of the main causes of inefficient reactant  
468 exploitation in the DTS, the alternative control strategy appears well suited to rationalise the  
469 use of the reactant, thus minimising the resulting generation of process residues.

470

### 471 **5.3 Results of the field test of the alternative control**

472 The alternative PI control was implemented in the DCS of the test facility. As outlined in  
473 section 4.4, a test run of the new control was carried out and the resulting operational data  
474 were compared with a previous period under the conventional process control configuration.  
475 The equivalence of action between the two controls was guaranteed by selecting the average  
476 value of outlet HCl concentration in the previous day under the conventional control as the  
477 setpoint for the test of the alternative control (see Fig. 7b).

478 Two 5-hour data samples with similar inlet flue gas conditions were selected for the  
479 comparative assessment. The two time series are shown in Fig. 7a, where it is possible to  
480 compare qualitatively the behaviour of the two control strategies, i.e. the feed rate of  
481 reactant and the outlet HCl flowrate, depending on the inlet HCl flowrate. The relative  
482 performance of the two controls was tracked via the indicators introduced in section 3.5.  
483 Table 1 provides the list of the indicators used and the specific values obtained, while Figure  
484 7c shows a radar plot comparing the normalised values of the performance indicators of the  
485 alternative control to the reference one. Internal normalisation was used to obtain the values  
486 shown in the figure. Given the low inlet SO<sub>2</sub> concentrations measured at the plant (in the

487 range 10 – 30 mg/Nm<sup>3</sup>) and the relatively low reactivity compared to HCl, the effect of SO<sub>2</sub> on  
488 system performance is negligible and not discussed in the analysis.

489 First of all, the two 5-hour data samples present highly comparable inlet HCl loads, hence the  
490 two controls are tested in a situation of similar stress. As reported in Table 1, the average inlet  
491 HCl mass flow rate in the two periods is equal and its CV is 68% higher during the test of the  
492 alternative control, i.e. the selection of data samples is slightly biased in favour of the  
493 conventional control.

494 Figure 7 shows that the real behaviour of the proposed PI-only control is in line with what was  
495 expected from the virtual simulation (see Fig. 6). The feed rate varies smoothly, with slow  
496 corrections in face of any sharp variation in the outlet HCl flow. Conversely, the conventional  
497 control reacts aggressively to deviations in the HCl outlet, with the characteristic spikes of  
498 reactant feed rate already described in Fig. 2.

499 When the performance indicators introduced in section 3.5 are considered, the parameter  
500 instability of reactant injection captures numerically this difference: while the commanded  
501 feed rate of the original control shows a CV that is 4.3 times higher than the CV of the inlet  
502 HCl molar flow, the CV of the commanded feed rate of the proposed control is only 1.24 times  
503 higher (a 71% reduction, see Table 1).

504 At the same time, the specific consumption of reactant in the Ca(OH)<sub>2</sub>-fed treatment stage is  
505 11% lower with the proposed control. This confirms that the lower aggressivity of the new  
506 control settings is not detrimental to the HCl removal efficiency of the system. On the  
507 contrary, in the test period, the proposed control managed to achieve the desired HCl  
508 removal performance with a significantly lower variability of reactant feed rate, which has the  
509 further advantage of reducing the mechanical stress to the screw feeder and the reactant  
510 transport system.



511 Another relevant metric is the instability of the outlet HCl flow, defined in section 3.5 as the  
512 ratio between the CVs of outlet and inlet HCl molar flow. The proposed PI-only control  
513 achieves a 39% reduction in this indicator. This means that the HCl load exiting the  $\text{Ca}(\text{OH})_2$ -  
514 fed treatment stage is less variable in time, thus the downstream  $\text{NaHCO}_3$ -fed stage operates  
515 on a less variable HCl inlet and is put in less stressful working conditions. As a consequence,  
516 the optimisation of the control in the  $\text{Ca}(\text{OH})_2$  stage generates also a 26% reduction in the  
517 specific consumption of reactant in the subsequent  $\text{NaHCO}_3$  stage (see again Table 1), whose  
518 control was not modified.

519 The overall consequence of the increase in efficiency owing to the new PI-only control is the  
520 reduction in the production of the solid process residues of HCl removal via both the gas-solid  
521 reactions with  $\text{Ca}(\text{OH})_2$  and  $\text{NaHCO}_3$ . The new control achieves a 7% and a 22% reduction in  
522 the generation of process residues, respectively in the 1<sup>st</sup> and 2<sup>nd</sup> treatment stages. The  
523 overall effect is a 13% reduction of the amount of process waste generated by the HCl removal  
524 operation. A further confirmation of this effect can be observed in figure S4 in the SI, which  
525 shows the simulated action of the conventional control system considering the inlet HCl load  
526 for the 5-hour dataset collected during the test-run. The figure evidences that the multiple  
527 activations of the feedback mode would have caused a higher reactant consumption.

528

#### 529 **5.4 Discussion**

530 In the light of the indicators in Table 1, the alternative control strategy tuned in the virtual  
531 simulation was demonstrated to improve the overall economic and environmental  
532 performance of the system. The consumption of reactants and the generation of process  
533 residues were lowered in both the treatment stages, by increasing the efficiency of reactant  
534 delivery. It was thus demonstrated that the main drawback of dry acid gas removal, i.e. the

535 required high excess of reactant, can be partially mitigated by introducing specific process  
536 control strategies. In particular, for a multistage system as that of the test facility, it is worth  
537 highlighting that an intervention limited to the 1<sup>st</sup> treatment stage can produce benefits also  
538 on the 2<sup>nd</sup> stage, by enabling a more efficient operation thanks to the lowered variability of  
539 the inlet HCl.

540 The alternative control strategy, based on a PI feedback control, however, has clear  
541 limitations: even if the simple feedback action reduces the variability of HCl load compared  
542 to the conventional control, the instability with respect to a setpoint is still quite high. More  
543 advanced control strategies could offer further improvements. Nonetheless, the proposed  
544 solution achieved the results in Table 1 with minimal need of full-scale testing and no  
545 significant change in the control architecture of the system, demonstrating the ease of  
546 implementation of better solid waste and reactant management via control optimisation.

547 The results obtained show that the procedure developed for the test of alternative control  
548 strategies, based on a virtual console, and the metric introduced, based on the performance  
549 indicators listed in Table 1, provide an effective approach to allow the improvement of the  
550 environmental and economic operational performance of acid gas treatment systems.

551

## 552 6 Conclusions

553 With increasingly strict limits on the emission of airborne pollutants as HCl, the flue gas  
554 treatment sections in WtE installations are experiencing problems of excessive consumption  
555 of reactants and related high generation of solid residues destined to landfilling, which lead  
556 to non-negligible indirect environmental burdens. By considering a reference state-of-the-art  
557 acid gas removal system, the present study demonstrated that a standard process control

558 approach based exclusively on the suppression of HCl emissions might be a suboptimal  
559 solution in terms of economic and environmental performance. A simple methodology based  
560 on virtual simulation and limited full-scale test-runs allowed identifying and tuning an  
561 alternative control strategy that achieved a reduction in the generation of solid process  
562 residues equal to 7% in the optimised  $\text{Ca}(\text{OH})_2$ -fed 1<sup>st</sup> stage of HCl removal and 13% in the  
563 overall two-stage treatment line with respect to the original control configuration, while  
564 maintaining the same HCl emission performance at stack.

565 Despite the relevant advantages in terms of reactant economy, a limitation of the proposed  
566 solution is that it only partially alleviates the fluctuations in the HCl concentration at the outlet  
567 of the 1<sup>st</sup> treatment stage, which are intrinsic to the WtE context. More advanced process  
568 control strategies, taking into account process disturbances other than inlet pollutant  
569 concentration and reactant feed rate, could be the key to develop plant-specific highly  
570 performant model-based control schemes. However, the present study evidenced that  
571 process control optimisation is a promising area of improvement in the management of WtE  
572 flue gas treatment, not only to improve stable operation, but also to increase significantly the  
573 economic and environmental performance of DSI processes without hindering the  
574 compliance to emission limits at stack.

575

576   References

- 577       Akinola, T.E., Oko, E., Gu, Y., Wei, H.-L., Wang, M., 2019. Non-linear system identification  
578       of solvent-based post-combustion CO<sub>2</sub> capture process. *Fuel* 239, 1213-1223.
- 579       Antonioni, G., Dal Pozzo, A., Guglielmi, D., Tugnoli, A., Cozzani, V., 2016. Enhanced  
580       modelling of heterogeneous gas-solid reactions in acid gas removal dry processes. *Chem.*  
581       *Eng. Sci.* 148, 140-154.
- 582       Ardolino, F., Boccia, C., Arena, U., 2020. Environmental performances of a modern waste-  
583       to-energy unit in the light of the 2019 BREF document. *Waste Manage.* 104, 94-103.
- 584       Arena, U., 2015. From waste-to-energy to waste-to-resources: The new role of thermal  
585       treatments of solid waste in the Recycling Society. *Waste Manage.* 37, 1-2.
- 586       Bagheri, M., Esfilar, R., Golchi, M.S., Kennedy, C.A., 2020. Towards a circular economy: A  
587       comprehensive study of higher heat values and emission potential of various municipal  
588       solid wastes. *Waste Manage.* 101, 210-221.
- 589       Bal, M., Reddy, T.T., Meikap, B.C., 2019. Removal of HCl gas from off gases using self-  
590       priming venturi scrubber. *J. Haz. Mat.* 364, 406-418.
- 591       Bazghaleh, M., Mohammadzaheri, M., Grainger, S., Cazzolato, B., Lu, T.-F., 2013. A new  
592       hybrid method for sensorless control of piezoelectric actuators. *Sensors and Actuators A:*  
593       *Physical* 194, 25-30.
- 594       Beylot, A., Hochar, A., Michel, P., Descat, M., Ménard, Y., Villeneuve, J., 2018. Municipal  
595       Solid Waste Incineration in France: An Overview of Air Pollution Control Techniques,  
596       Emissions, and Energy Efficiency. *J. Ind. Ecol.* 22, 1016-1026.
- 597       Bogush, A., Stegemann, J.A., Wood, I., Roy, A., 2015. Element composition and  
598       mineralogical characterisation of air pollution control residue from UK energy-from-waste  
599       facilities. *Waste Manage.* 36, 119-129.
- 600       CEN, 2019. CEN/TS 17337:2019 – Stationary source emissions - Determination of mass  
601       concentration of multiple gaseous species - Fourier transform infrared spectroscopy.  
602       European Committee for Standardization, Bruxelles, Belgium.
- 603       Choi, S., Yoo, C., Lee, I.-B., 2002. SO<sub>x</sub> monitoring and neural net classification in the power  
604       plant. *J. Environ. Eng.* 128, 911-918.
- 605       Cignitti, S., Mansouri, S.S., Sales-Cruz, M., Jensen, F., Huusom, J.K., 2016. Dynamic  
606       Modeling and Analysis of an Industrial Gas Suspension Absorber for Flue Gas  
607       Desulfurization. *Emiss. Control Sci. Technol.* 2, 20-32.
- 608       Coleman, M.D., Ellison, M., Robinson, R.A., Gardiner, T.D., Smith, T.O.M., 2019.  
609       Uncertainty requirements of the European Union’s Industrial Emissions Directive for  
610       monitoring sulfur dioxide emissions: Implications from a blind comparison of sulfate  
611       measurements by accredited laboratories. *J. Air Waste Manage. Assoc.* 69, 1070-1078.
- 612       Dal Pozzo, A., Moricone, R., Tugnoli, A., Cozzani, V., 2019. Experimental Investigation of  
613       the Reactivity of Sodium Bicarbonate toward Hydrogen Chloride and Sulfur Dioxide at Low  
614       Temperatures. *Ind. Eng. Chem. Res.* 58, 6316-6324.

615 Dal Pozzo, A., Lazazzara, L., Antonioni, G., Cozzani, V., 2020. Techno-economic  
616 performance of HCl and SO<sub>2</sub> removal in waste-to-energy plants by furnace direct sorbent  
617 injection. *J. Haz. Mat.* 394, 122518.

618 Dal Pozzo, A., Guglielmi, D., Antonioni, G., Tugnoli, A., 2018a. Environmental and  
619 economic performance assessment of alternative acid gas removal technologies for  
620 waste-to-energy plants. *Sust. Prod. Consumption* 16, 202-215.

621 Dal Pozzo, A., Armutlulu, A., Rekhtina, M., Müller, C.R., Cozzani, V. 2018b. CO<sub>2</sub> Uptake  
622 Potential of Ca-Based Air Pollution Control Residues over Repeated Carbonation-  
623 Calcination Cycles. *Energy Fuels* 32, 5386-5395.

624 Dal Pozzo, A., Giannella, M., Antonioni, G., Cozzani, V., 2018c. Optimization of the  
625 economic and environmental profile of HCl removal in a municipal solid waste incinerator  
626 through historical data analysis. *Chem. Eng. Trans.* 67, 463-468.

627 Dal Pozzo, A., Guglielmi, D., Antonioni, G., Tugnoli, A., 2017. Sustainability analysis of dry  
628 treatment technologies for acid gas removal in waste-to-energy plants. *J. Clean. Prod.* 162,  
629 1061-1074.

630 Dal Pozzo, A., Antonioni, G., Guglielmi, D., Stramigioli, C., Cozzani, V., 2016. Comparison  
631 of alternative flue gas dry treatment technologies in waste-to-energy processes. *Waste*  
632 *Manage.* 51, 81-90.

633 Damgaard, A., Riber, C., Fruergaard, T., Hulgaard, T., Christensen, T.H., 2010. Life-cycle-  
634 assessment of the historical development of air pollution control and energy recovery in  
635 waste incineration. *Waste Manage.* 30, 1244-1250.

636 De Greef, J., Villani, K., Goethals, J., Van Belle, H., Van Caneghem, J., Vandecasteele, C.,  
637 2013. Optimising energy recovery and use of chemicals, resources and materials in  
638 modern waste-to-energy plants. *Waste Manage.* 33, 2416-2424.

639 Dong, J., Jeswani, H.K., Nzihou, A., Azapagic, A., 2020. The environmental cost of  
640 recovering energy from municipal solid waste. *Appl. Energy* 267, 114792.

641 Ephraim, A., Ngo, L.D., Pham Minh, D., Lebonnois, D., Peregrina, C., Sharrock, P., Nzihou,  
642 A., 2019. Valorization of Waste-Derived Inorganic Sorbents for the Removal of HCl in  
643 Syngas. *Waste Biomass Valorization* 10, 3435-3446.

644 Foo, R., Berger, R., Heiszwolf, J.J., 2016. Reaction Kinetic Modeling of DSI for MATS  
645 Compliance. In: Proceedings of the Power Plant Pollutant Control and Carbon  
646 Management "MEGA" Symposium, Baltimore, MD, USA, 16–19 August 2016

647 Gassner, M., Nilsson, J., Nilsson, E., Palmé, T., Züfle, H., Bernero, S., 2014. A data-driven  
648 approach for analysing the operational behaviour and performance of an industrial flue  
649 gas desulphurisation process. *Computer Aided Chem. Eng.* 33, 661-666.

650 Gerassimidou, S., Velis, C.A., Williams, P.T., Castaldi, M.J., Black, L., Komilis, D., 2020.  
651 Chlorine in waste-derived solid recovered fuel (SRF), co-combusted in cement kilns: A  
652 systematic review of sources, reactions, fate and implications. *Critical Reviews in*  
653 *Environmental Science and Technology*, in press.

654 Goodall, P.; Sharpe, R.; West, A., 2019. A data-driven simulation to support  
655 remanufacturing operations. *Computers in Industry* 105, 48-60.

656 Guo, Y., Xu, Z., Zheng, C., Shu, J., Dong, H., Zhang, Y., Weng, W., Gao, X., 2019. Modeling  
657 and optimization of wet flue gas desulfurization system based on a hybrid modeling  
658 method. *J. Air Waste Manage. Assoc.* 69, 565-575.

659 Gutiérrez Ortiz, F.J., Ollero, P., 2008. A realistic approach to modeling an in-duct  
660 desulfurization process based on an experimental pilot plant study. *Chem. Eng. J.* 141,  
661 141-150.

662 Harriott, P., 1990. A Simple Model for SO<sub>2</sub> Removal in the Duct Injection Process. *J. Air  
663 Waste Manage. Assoc.* 40, 998-1003.

664 Hartman, M., Svoboda, K., Pohorely, M., Syc, M., 2013. Thermal Decomposition of Sodium  
665 Hydrogen Carbonate and Textural Features of Its Calcines. *Ind. Eng. Chem. Res.* 52, 10619-  
666 10626.

667 Hunt, G., Sewell, M., 2015. Utilizing Dry Sorbent Injection Technology to Improve Acid Gas  
668 Control. In: 34th International Conference on Thermal Treatment Technologies &  
669 Hazardous Waste Combustors, Houston, TX, USA, 20-22 October 2015

670 Iizuka, A., Morishita, Y., Shibata, E., Takatoh, C., Cho, H., 2020. Basic Study of the Reaction  
671 of Calcium Hydroxide with Hydrogen Chloride Using Single Crystals. *Ind. Eng. Chem. Res.*  
672 59, 9699-9704.

673 Kameda, T., Tochinai, M., Kumagai, S., Yoshioka, T., 2020. Treatment of HCl gas by cyclic  
674 use of Mg–Al layered double hydroxide intercalated with CO<sub>3</sub><sup>2-</sup>. *Atmospheric Pollution  
675 Res.* 11, 290-295.

676 Kim, K.-D., Jeon, S.-M., Hasolli, N., Lee, K.-S., Lee, J.-R., Han, J.-W., Kim, H.T., Park, Y.-O.,  
677 2017. HCl removal characteristics of calcium hydroxide at the dry-type sorbent reaction  
678 accelerator using municipal waste incinerator flue gas at a real site. *Korean J Chem Eng*  
679 34, 747-756.

680 Kockmann, N., 2019. Digital methods and tools for chemical equipment and plants. *Reaction  
681 Chemistry and Engineering* 4, 1522-1529.

682 Lausset, C., Cherubini, F., del Alamo Serrano, G., Becidan, M., Strømman, A.H., 2016.  
683 Life-cycle assessment of a Waste-to-Energy plant in central Norway: Current situation and  
684 effects of changes in waste fraction composition. *Waste Manage.* 58, 191-201.

685 Liu, T., Gao, F., 2012. Step Response Identification of Stable Processes. In: Liu, T., Gao, F.,  
686 Industrial Process Identification and Control Design, Springer-Verlag London, London, UK.

687 Liu, S., Sun, L., Zhu, S., (...), Chen, X., Zhong, W., 2020. Operation strategy optimization of  
688 desulfurization system based on data mining. *Appl. Mathematical Modelling* 81, 144-158.

689 Ljung, L., 2010. Perspectives on system identification. *Annual Reviews in Control* 34, 1-12.

690 Margallo, M., Taddei, M.B.M., Hernández-Pellón, A., Aldaco, R., Irabien, A., 2015.  
691 Environmental sustainability assessment of the management of municipal solid waste  
692 incineration residues: A review of the current situation. *Clean Technol. Environ. Policy* 17,  
693 1333-1353.

694 Montagnaro, F., Balsamo, M., Salatino, P., 2016. A single particle model of lime sulphation  
695 with a fractal formulation of product layer diffusion. *Chem. Eng. Sci.* 156, 115-120.

696 Muratori, G., Dal Pozzo, A., Antonioni, G., Cozzani, V., 2020. Application of Multivariate  
697 Statistical Methods to the Modelling of a Flue Gas Treatment Stage in a Waste-to-energy  
698 Plant. *Chem. Eng. Trans.* 82, 397-402.

699 Nelles, O., 2020. Nonlinear System Identification: From Classical Approaches to Neural  
700 Networks, Fuzzy Models, and Gaussian Processes. Springer Nature, Berlin, Germany.

701 Neuwahl, F., Cusano, G., Gomez Benavides, J., Holbrook, S., Roudier, S., 2019. Best  
702 Available Techniques (BAT) Reference Document for Waste Incineration. EUR 29971 EN.  
703 doi:10.2760/761437

704 Ouda, O.K.M., Raza, S.A., Nizami, A.S., Rehan, M., Al-Waked, R., Korres, N.E., 2016. Waste  
705 to energy potential: A case study of Saudi Arabia. *Renewable Sustainable Energy Reviews*  
706 61, 328-340.

707 Peng, H., Ozaki, T., Toyoda, Y., Shioya, H., Nakano, K., Haggan-Ozaki, V., Mori, M., 2004.  
708 RBF-ARX model-based nonlinear system modeling and predictive control with application  
709 to a NO<sub>x</sub> decomposition process. *Control Engineering Practice* 12, 191-203.

710 Quina, M.J., Bontempi, E., Bogush, A., Schlumberger, S., Weibel, G., Braga, R., Funari, V.,  
711 Hyks, J., Rasmussen, E., Lederer, J., 2018. Technologies for the management of MSW  
712 incineration ashes from gas cleaning: New perspectives on recovery of secondary raw  
713 materials and circular economy. *Sci. Total Environ.* 635, 526-542.

714 Saleem, M., Krammer, G., 2012. On the Stability of Pulse-Jet Regenerated-Bag Filter  
715 Operation. *Chemical Engineering and Technology* 35, 877-884.

716 Smrekar, J., Potočnik, P., Senegačnik, A., 2013. Multi-step-ahead prediction of NO<sub>x</sub>  
717 emissions for a coal-based boiler. *Appl. Energy* 106, 89-99.

718 Ting, C.-H., Chen, H.-H., Yen, C.-C., 2008. A PID ratio control for removal of HCl/SO<sub>x</sub> in flue  
719 gas from refuse municipal incinerators. *Control Engineering Practice* 16, 286-293.

720 Van Caneghem, J., Van Acker, K., De Greef, J., Wauters, G., Vandecasteele, C., 2019.  
721 Waste-to-energy is compatible and complementary with recycling in the circular  
722 economy. *Clean Technol. Environ. Policy*, in press.

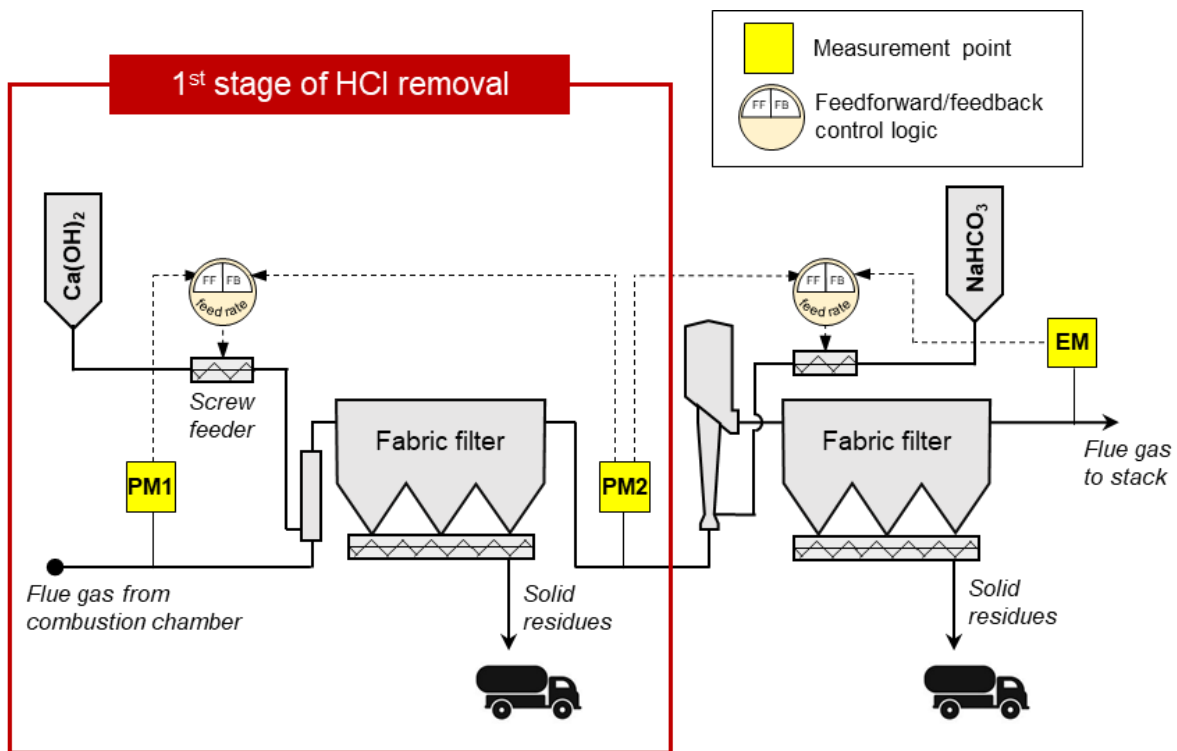
723 Vehlow, J., 2015. Air pollution control systems in WtE units: An overview. *Waste Manage.*  
724 37, 58-74.

725 Wu, C., Kang, S.-J., Keener, T.C., Lee, S.-K., 2004. A model for dry sodium bicarbonate duct  
726 injection flue gas desulfurization. *Advances in Environmental Research* 8, 655-666.

727 Yang, N., Damgaard, A., Scheutz, C., Shao, L.-M., He, P.-J., 2018. A comparison of chemical  
728 MSW compositional data between China and Denmark. *J. Environ. Sci.* 74, 1-10.

729 Zhang, H., Yu, S., Shao, L., He, P., 2019. Estimating source strengths of HCl and SO<sub>2</sub>  
730 emissions in the flue gas from waste incineration. *J. Environ. Sci.* 75, 370-377.

731  
732  
733  
734  
735

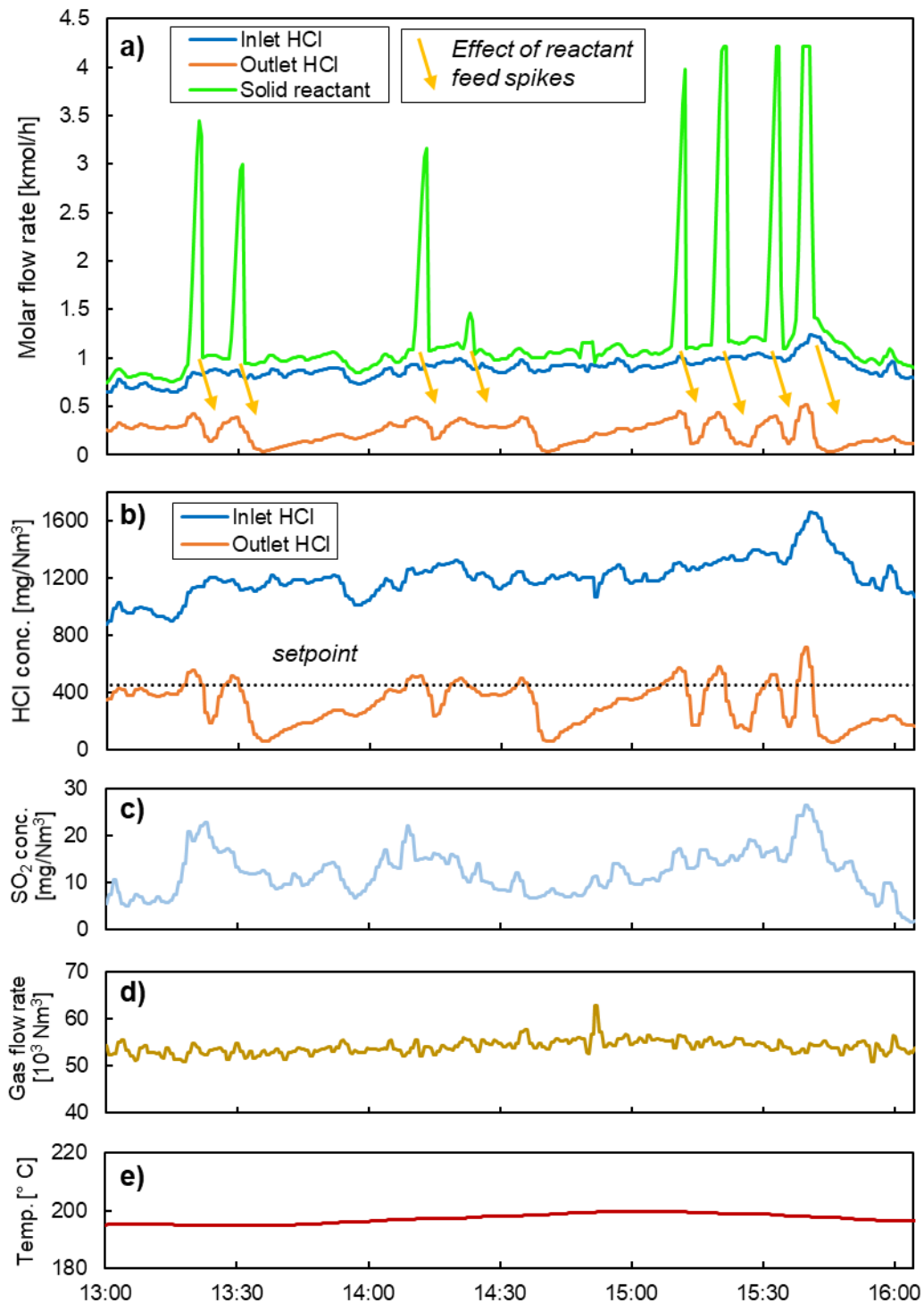


738

739 **Figure 1.** Scheme of the two-stage acid gas abatement system of the test facility considered,  
 740 including measurement points of flue gas composition (PM1, PM2 = process measurement,  
 741 EM = measurement at stack) and control loops for reactant feed rate. Control optimization of  
 742 1<sup>st</sup> stage (red box in the figure) was the object of the study.

743

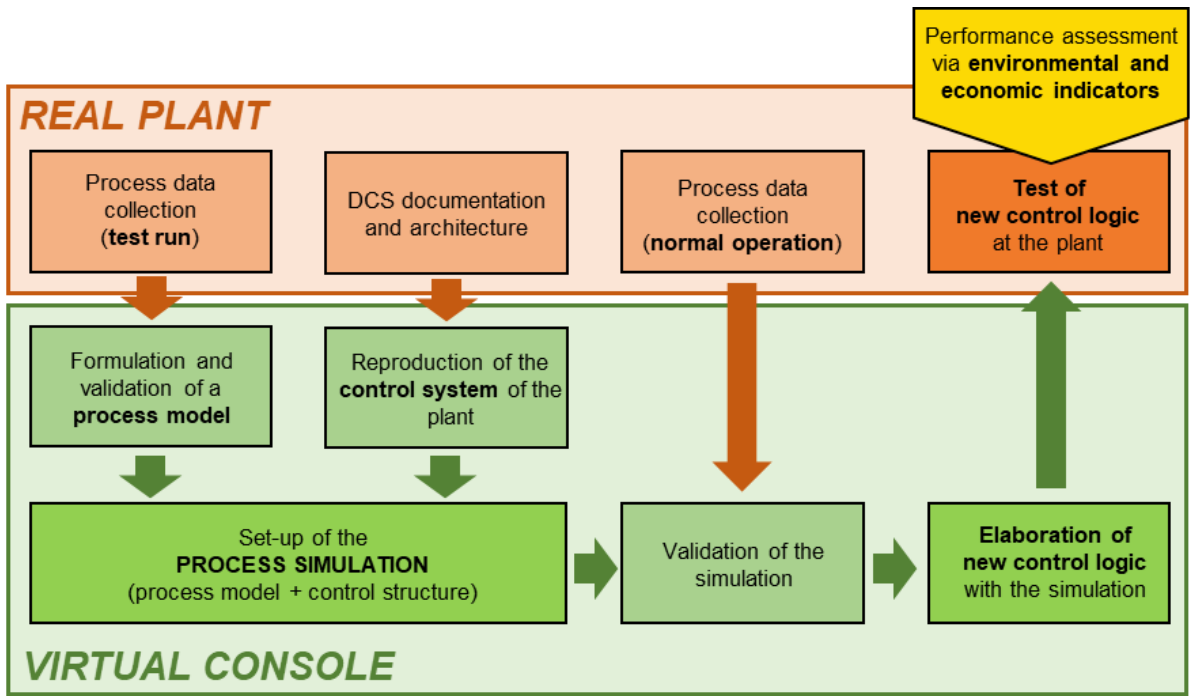




744

745 **Figure 2.** Data recorded by the distributed control system (DCS) of an Italian WtE facility  
 746 showing: a) the typical trend of inlet and outlet HCl flowrate and solid reactant feed rate  
 747 during normal operation of the 1<sup>st</sup> stage acid gas removal unit applying the conventional  
 748 process control strategy; b) threshold setpoint with respect to HCl inlet and outlet  
 749 concentrations; c) SO<sub>2</sub> concentration; d) flue gas flowrate; e) operating temperature.

750



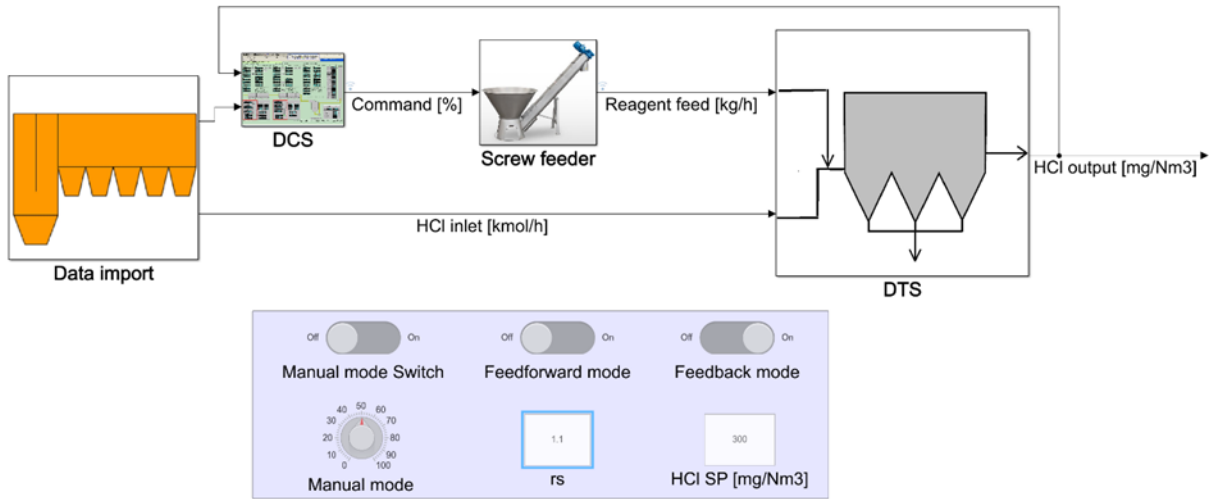
751

752 **Figure 3.** Methodology developed for testing and tuning of improved process control

753 strategies.

754

755

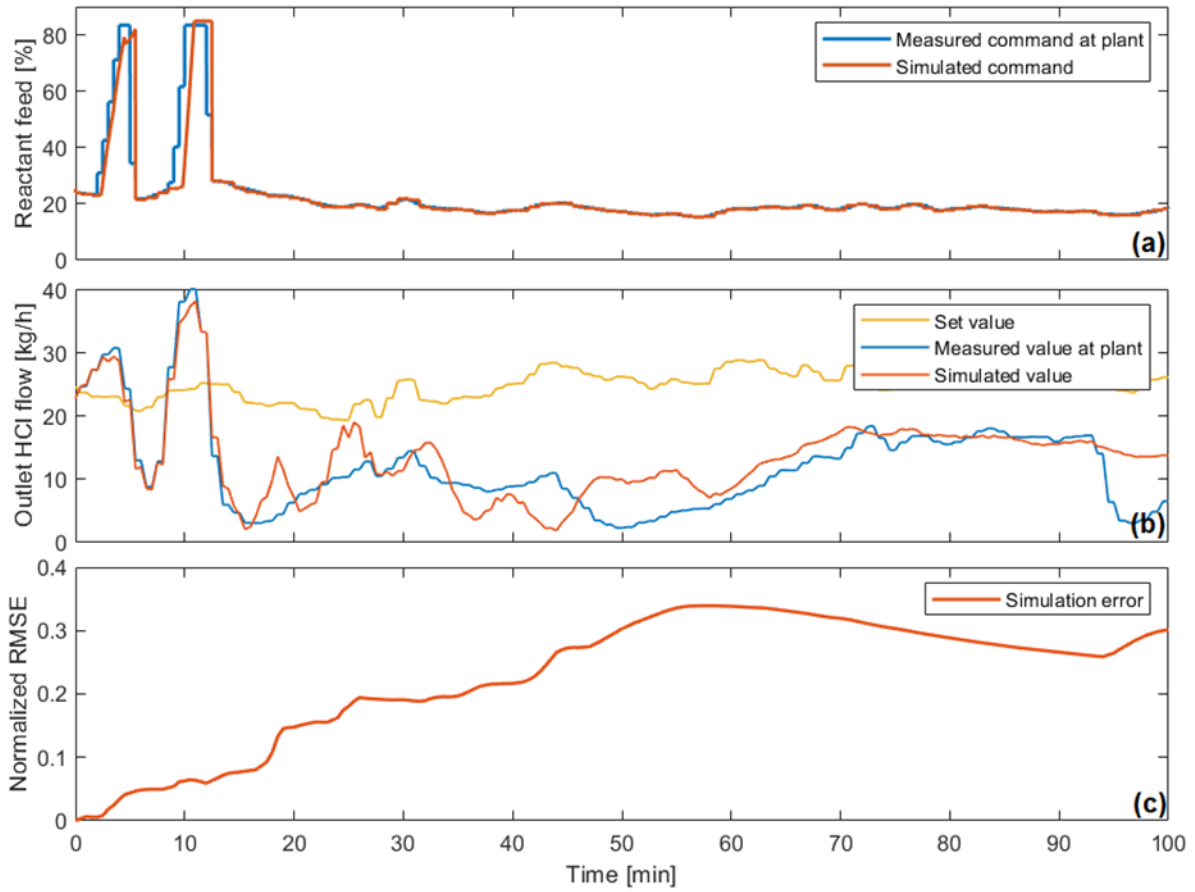


756

757 **Figure 4.** Virtual console developed to simulate the DSI process (1<sup>st</sup> stage of the acid gas

758 removal system in Fig. 1) using the Simulink<sup>®</sup> software tool.

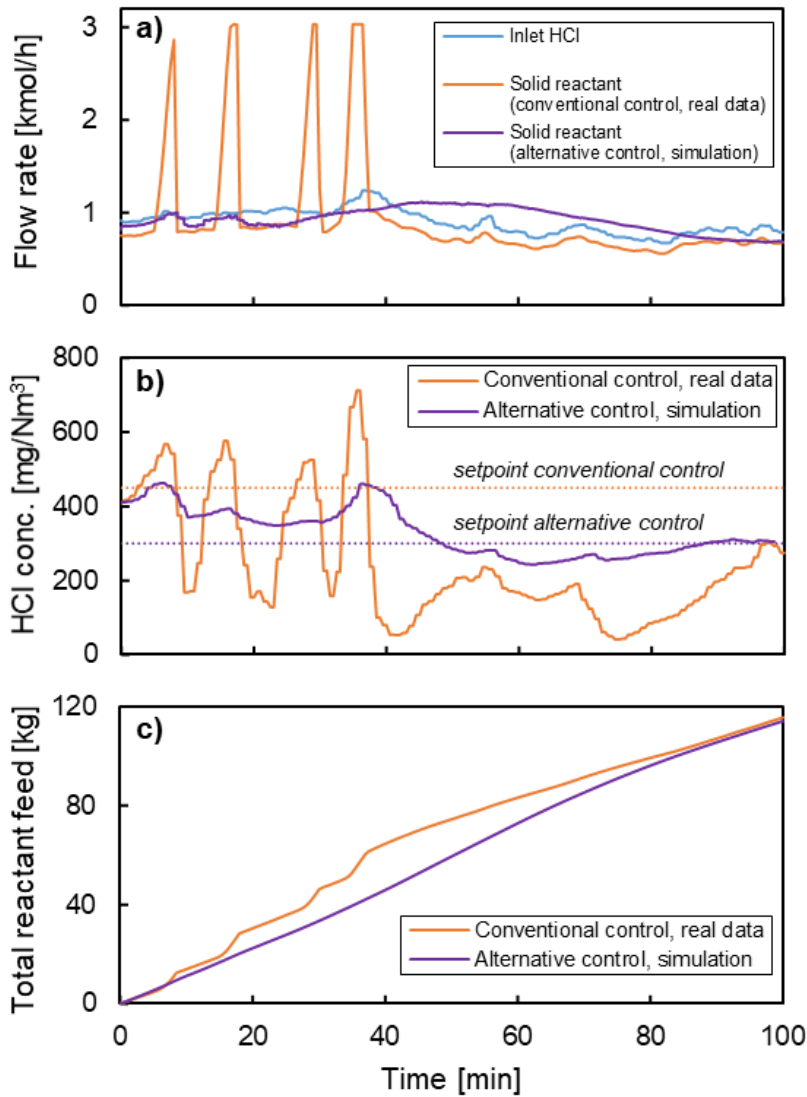
759



760  
761

762 **Figure 5.** Performance of the virtual console in simulating the behaviour of the conventional  
 763 control of the system: a) measured vs. simulated command of reactant feed, b) measured vs.  
 764 simulated outlet HCl flow rate, compared to the set value of the control, c) cumulative average  
 765 error of the simulation.

766



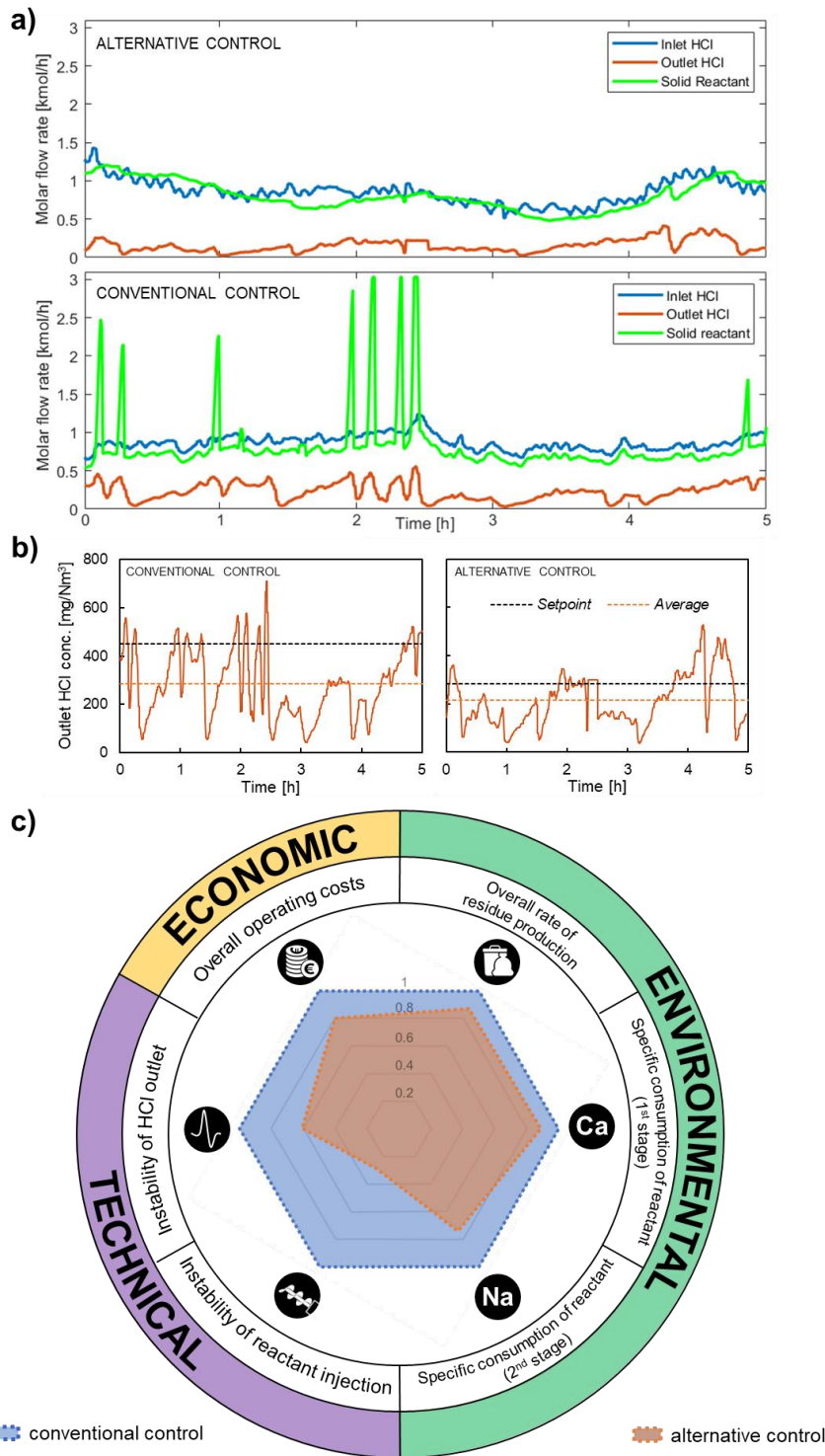
767

768 **Figure 6.** a) Simulation of the reactant feed rate by the alternative PI control strategy

769 compared to the conventional process control on a sample dataset; b) deviation of the outlet

770 HCl concentration from the respective setpoints, c) resulting cumulated reactant consumption.

771



778 **Table 1.** Performance of the alternative control strategy vs. the conventional process control  
 779 monitored according to the performance indicators introduced in section 3.5.

Parameter or indicator		Test period		$\Delta$
		Conventional control	Alternative control	
Inlet HCl mass flow rate (kg/h)	$\mu$	64.4	64.4	-
	CV	0.12	0.19	+68%
Feed rate of reactant, Ca(OH) <sub>2</sub> (kg/h)	$\mu$	61.1	60.0	-2%
	CV	0.49	0.24	-52%
Outlet HCl mass flow rate (kg/h)	$\mu$	17.2	12.5	-27%
	CV	0.51	0.52	+2%
HCl removal efficiency (%)	$\mu$	75.8	82.3	+9%
	CV	11.2	8.5	-24%
<b>Instability of reactant injection</b> (CV of Ca(OH) <sub>2</sub> feed rate / CV of inlet HCl)		4.27	1.24	<b>-71%</b>
<b>Instability of HCl outlet</b> (CV of outlet HCl / CV of inlet HCl)		4.4	2.7	<b>-39%</b>
<b>Specific consumption of reactant</b> (1 <sup>st</sup> stage) (kg of Ca(OH) <sub>2</sub> fed / kg of HCl removed)		1.30	1.16	<b>-11%</b>
<b>Specific generation of residues</b> (1 <sup>st</sup> stage) (kg of residues / kg of HCl removed)		1.80	1.67	<b>-7%</b>
<b>Specific consumption of reactant</b> (2 <sup>nd</sup> stage) (kg of NaHCO <sub>3</sub> fed / kg of HCl removed)		3.85	2.86	<b>-26%</b>
<b>Specific generation of residues</b> (2 <sup>nd</sup> stage) (kg of residues / kg of HCl removed)		2.55	2.00	<b>-22%</b>
<b>Overall rate of residue production</b> (kg of residues / kg of HCl removed)		2.00	1.73	<b>-13%</b>
<b>Overall economic performance</b> (€ of operating costs / kg of HCl removed)		1.86	1.48	<b>-20%</b>

780

781

1 Economic and environmental benefits by improved process control strategies in HCl removal  
2 from waste-to-energy flue gas

3

4 *Alessandro Dal Pozzo, Giacomo Muratori, Giacomo Antonioni, Valerio Cozzani\**

5 LISES - Dipartimento di Ingegneria Civile, Chimica, Ambientale e dei Materiali, Alma Mater  
6 Studiorum - Università di Bologna, via Terracini n.28, 40131 Bologna, Italy

7

8 (\*)*corresponding author*, Tel. +39-051-2090240, Fax +39-051-2090247, e-mail:  
9 valerio.cozzani@unibo.it

10

11 **Abstract**

12 The control of HCl emission in waste-to-energy (WtE) facilities is a challenging flue gas  
13 treatment problem: the release of HCl from waste combustion is highly variable in time and  
14 the HCl emission standards are typically far lower in WtE than in any other industry.  
15 Traditional process control approaches in dry HCl removal processes are generally based on  
16 feeding a large excess of solid reactants to the system, to ensure robustness and a wide safety  
17 margin in the compliance to environmental regulations. This results in the production of a  
18 high amount of unreacted sorbents, strongly increasing the generation of solid wastes that  
19 need to be disposed. *In the present study, an approach was developed to allow the*  
20 *implementation of improved control strategies for dry HCl abatement systems in operating*  
21 *full-scale facilities. Its objective is the reduction of the reactant feed and the waste*  
22 *production, while still providing an adequate safety margin for emission compliance. The*  
23 *approach was based on the reproduction of the behaviour of the real system in a virtual*  
24 *console that allows the extensive testing of alternative control strategies, limiting the need of*  
25 *demanding test-runs at the real plant. A test case on an Italian WtE facility demonstrated the*  
26 *capability of a control logic tuned in the virtual console to achieve a 13% reduction in the*  
27 *consumption of reactants and generation of process residues, with unchanged HCl removal*



28 **efficiency.** The results evidence the wide opportunities for optimisation of dry acid gas  
29 removal systems, in particular when multistage systems are implemented.

30 **Keywords:** waste-to-energy, HCl, process optimization, dry sorbent injection.

## 31 1 Introduction

32 In a modern waste management system, waste-to-energy (WtE) facilities have the role to  
33 divert from landfilling waste streams for which recycling is currently technically or  
34 economically unfeasible (Nizami et al., 2016) and enabling their thermal valorisation (Arena  
35 et al., 2015), thus facilitating the transition to a circular economy (Bagheri et al., 2020; Van  
36 Caneghem et al., 2019). Thanks to increasingly ambitious environmental regulations, the  
37 emission of several air pollutants related to WtE operation has been reduced more than  
38 tenfold in the last decades (Ardolino et al., 2020; Damgaard et al., 2010). However, in the  
39 current holistic approach to environmental protection, the reduction of impacts has to go  
40 beyond the minimisation of the emission of pollutants at the stack of the plant. Also indirect  
41 impacts, e.g. those associated to the consumption of reactants and the production of process  
42 residues in the flue gas treatment system of the plant (Dal Pozzo et al., 2017; Dong et al.,  
43 2020; Lousselet et al., 2016), needs to be minimised.

44 Hydrogen chloride (HCl) is a typical pollutant in WtE flue gases, arising from the combustion  
45 of waste containing chlorine (Zhang et al., 2019). Chlorine is widely dispersed amongst organic  
46 and inorganic compounds present in several waste items (Gerassimidou et al., 2020; Yang et  
47 al., 2018). Among the different techniques available for HCl removal (Bal et al., 2019; Dal  
48 Pozzo et al., 2019; Ephraim et al., 2019; Kameda et al., 2020), dry sorbent injection (DSI) is  
49 one of the technologies more frequently implemented (Beylot et al., 2018; Dal Pozzo et al.,  
50 2018a). DSI consists in the in-duct addition of an alkaline powdered reactant (e.g. calcium

51 hydroxide or sodium bicarbonate), which neutralises acid pollutants as HCl via gas-solid  
52 reaction (Antonioni et al., 2016). DSI, adopted in either single or two-stage configurations (Dal  
53 Pozzo et al., 2016; De Greef et al., 2013), is considered among the best available techniques  
54 for flue gas treatment in WtE installations recommended by the European Union (Neuwahl et  
55 al., 2019).

56 The main environmental drawback of DSI systems is the high stoichiometric excess of reactant  
57 feed that is required to achieve high HCl removal efficiency (Vehlow, 2015). The resulting  
58 excess consumption of reactant leads to the generation of relevant streams of solid **process**  
59 **residues in the fabric filters, where they are collected together with fly ashes and**  
60 **micropollutants. The presence of these other components in the collected process residues**  
61 **causes the stream to be considered as hazardous waste and to require its disposal in**  
62 **dedicated landfill sites (Dal Pozzo et al., 2018b; Kameda et al., 2020).**

63 **In addition, given that the composition of the waste burnt in the combustion chamber of a**  
64 **WtE plant varies widely over time, the resulting extreme variability of HCl concentration at**  
65 **the inlet of the flue gas treatment section (Dal Pozzo et al., 2020) is an inherent instability**  
66 **that limits the effectiveness of conventional control strategies in calibrating the reactant feed**  
67 **needed to maintain a constant concentration setpoint at the outlet. Thus, the prevailing trend**  
68 **in control strategies is to calibrate the process control parameters of the DSI system on the**  
69 **safe side, and even more so accept high excess feed rates of reactants to minimise the**  
70 **possible occurrence of overruns of HCl emission limits at stack.**

71 **A more accurate setting of the DSI control system could ensure not only a safe compliance of**  
72 **emission limits at stack, but also a reduction of the consumption of reactants and the**  
73 **generation of process residues. These in principle represent an undesired environmental**

74 **burden shift between different compartments (from air to soil/water) (Bogush et al., 2015;**  
75 **Margallo et al., 2015; Quina et al., 2018).**

76 The problem of the optimisation of flue gas treatment control with reference either to the  
77 WtE context or to acid pollutants (HCl, SO<sub>2</sub>, HF) is scarcely addressed in scholarly literature.  
78 Ting et al. (2008) described the design of a PID control for acid gas removal via semi-dry  
79 scrubbing in a WtE plant, with parameter tuning performed during commissioning operation.  
80 Gassner et al. (2014) explored the use of data-driven modelling approaches to describe the  
81 non-stationary operational behaviour of a semi-dry flue gas desulfurization process. Cignitti  
82 et al. (2016) developed a simple first principle model to predict the dynamics of a semidry SO<sub>2</sub>  
83 absorber in desulfurization units of coal-fired power plants, while Guo et al. (2019) used a  
84 hybrid approach, blending first principles and neural network, to model and optimise a wet  
85 flue gas desulfurization unit. Yet, the focus of these recent studies has been mainly the  
86 theoretical development of enhanced dynamic models of the process, rather than their  
87 implementation in real control schemes. In particular, to the best of the authors' knowledge,  
88 no previous paper addresses the potential environmental and economic advantages in terms  
89 of reduced reactant consumption and related waste generation achievable with process  
90 control optimisation in WtE acid gas removal.

91 Furthermore, control optimisation in the WtE context is made complex by the fact that  
92 conventional direct tuning via extensive test runs during plant operation is generally  
93 incompatible with the need to comply with strict HCl emission limits in presence of a highly  
94 variable inlet load of HCl coming from waste combustion. In this regard, the set-up of data-  
95 driven simulations of the real system in a virtual environment, as more and more frequently  
96 performed in the manufacturing (Goodall et al., 2019) and process industry (Kockmann,  
97 2019), could drastically reduce the need of field tests. By this strategy, the screening and the

98 tuning of new control settings is carried out directly in a virtual set-up, thus limiting the  
99 number of in-field test runs only to those needed for the initial calibration of the simulation  
100 and for the final trial of the new control system.

101 The present study focuses on the development of an approach for the optimisation of process  
102 control in a typical DSI system for HCl removal based on a virtual environment. A dynamic  
103 simulation of the dry treatment system was built in a virtual console implemented using the  
104 Simulink software. A data-driven process model, calibrated with a specific set of test data,  
105 nested into a reproduction of the control system of the DSI unit, was thus obtained and  
106 validated. The virtual console was used to test and tune an alternative control strategy, with  
107 the objective to reduce the stoichiometric excess of reactant associated to HCl removal. The  
108 alternative control was then tested in full scale at the real plant, demonstrating the potential  
109 for significant environmental and economic benefits deriving from the reduction in reactant  
110 consumption and related process waste generation.

111

## 112 2 Reference system and test facility

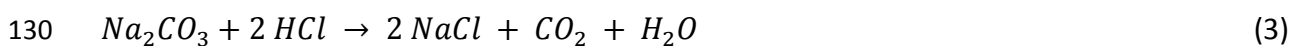
113

### 114 2.1 HCl removal system

115 The two-stage acid gas abatement system of a medium-sized (400 t/d of waste treated) WtE  
116 facility located in Northern Italy was used as case study. As shown in Fig. 1, this system is  
117 based on two consecutive steps of dry sorbent injection and filtration, taking place at ~180  
118 °C, downstream of the heat recovery section of the plant. In the first stage, calcium hydroxide,  
119 Ca(OH)<sub>2</sub>, is injected, triggering the following gas-solid reaction of HCl neutralisation (Iizuka et  
120 al., 2020):



122 A fabric filter separates the solid product of reaction from the flue gas, together with a  
123 relevant unreacted fraction of Ca(OH)<sub>2</sub>, present both due to the excess feed of reactant and  
124 for the intrinsic diffusional limitations of gas-solid reaction (i.e. the phenomenon of  
125 incomplete conversion discussed by Antonioni et al., 2016). In the second stage, the dry  
126 injection is based on sodium bicarbonate, NaHCO<sub>3</sub>. At the injection temperature and, in  
127 general, at T > 130 °C (see Hartman et al., 2013), NaHCO<sub>3</sub> decomposes to porous sodium  
128 carbonate (Na<sub>2</sub>CO<sub>3</sub>), which in turn absorbs HCl (Dal Pozzo et al., 2019):



131 Again, the solid product of reaction and an unreacted fraction of reactant are collected by a  
132 fabric filter. This two-stage configuration is adopted in several European WtE installations and  
133 it is appreciated for its built-in redundancy in terms of emission control (De Greef et al., 2013)  
134 and its flexibility that allows different repartitions of abatement demand between the two  
135 stages (Dal Pozzo et al., 2016).

136 As shown in Fig. 1, the present study is focused on the optimisation of the control of the  
137  $\text{Ca(OH)}_2$  1<sup>st</sup> stage of acid gas removal, referred to in the following as dry sorbent injection (DSI)  
138 system. As discussed in the following, the optimisation and tuning of the process control of  
139 the 1<sup>st</sup> stage not only improves the performance of the stage, but, stabilising the HCl outlet  
140 concentration, it also favours the optimal performance of the 2<sup>nd</sup> stage.

141

## 142 **2.2 Process control**

143 In the test facility, a conventional process control scheme implemented in several similar  
144 plants is present. The operation of the two-stage acid gas abatement system is monitored by  
145 the continuous acquisition of flue gas composition data at the measurement points PM1, PM2  
146 and EM indicated in Fig. 1. **The concentration of the main gas species at the sampling points,**  
147 **including the acid pollutants (HCl, SO<sub>2</sub>, HF), is measured by Fourier-Transform infrared (FTIR)**  
148 **spectrometry, in compliance with CEN/TS 17337 (CEN, 2019), while the flue gas flowrate is**  
149 **determined at stack (point EM) by means of S-type Pitot tube velocity measurements.**

150 In both the acid gas abatement stages, the distributed control system (DCS) of the plant  
151 controls the solid reactant feed based on the measured inlet and outlet mass flowrates of  
152 acid pollutants. A conditional logic selects the reactant feed rate as the maximum of two  
153 values, calculated as follows:

- 154 i. *Feedforward criterion.* The calculated feed rate is equal to the stoichiometric demand  
155 related to the abatement of the inlet mass flowrates of acid pollutants at PM1,  
156 increased by a 10% excess.
- 157 ii. *Feedback criterion.* The feed rate is calculated according to a Proportional Integral (PI)  
158 feedback formula based on the difference between a set-point for the outlet HCl  
159 concentration and the value measured at PM2.

160 The settings of the feedback control (proportional gain  $K_p = 5$  and integral gain  $\tau_I = 8$  s)  
161 provide an aggressive reaction, i.e. strong excess feed rates of reactant are delivered  
162 whenever the outlet HCl concentration exceeds the setpoint. Conversely, when the outlet HCl  
163 concentration is lower than the setpoint, the feed rate of reactant does not drop as  
164 significantly, because the feedforward criterion takes over. Thus, the combination of the  
165 feedforward and feedback criteria as detailed above realises an asymmetrical control action,  
166 in which the setpoint is actually treated as a threshold. The feedforward PI control works  
167 merely as an environmental safeguard, intended to act only if the feedforward is not capable  
168 to maintain the outlet below the given threshold. A survey carried out by the authors involving  
169 several Italian companies (HERAmbiente, HestAmbiente, IREN, Brianza Energia Ambiente)  
170 evidenced that this control strategy is typical of WtE acid gas abatement units, as the  
171 objective is to avoid any spike in outlet HCl resulting from a variation in the inlet HCl load  
172 coming from waste combustion (Muratori et al., 2020).

173

### 174 **2.3 Drawbacks of the reference control system**

175 The typical behaviour of the control system described in section 2.2 is shown in Fig. 2. Most  
176 of the time the control operates in feedforward mode and the feed rate of solid reactant is  
177 proportional to the inlet HCl load. However, when the outlet HCl flowrate exceeds its setpoint,  
178 the feedback mode takes over, imposing a relevant excess in feed rate to bring the HCl outlet  
179 back under the threshold as soon as possible. This behaviour determines a peak in reactant  
180 consumption but generates also unintended instability in the outlet HCl flow rate. As  
181 pinpointed by the arrows in Fig. 2, the spike of reactant feed manages to quickly reduce the  
182 outlet HCl flow rate, but such a reduction is often followed by a swift rebound of outlet HCl  
183 to high values that triggers another activation of the feedback control, resulting in another

184 spike of reactant feed. Since the layers of solid reactant accumulated over time on the fabric  
185 filter are known to play a major role in the overall acid gas removal action (Kim et al., 2017;  
186 Wu et al., 2004), the spikes of reactant feed might be detrimental because they induce  
187 unstable operation of the filter (Saleem and Krammer, 2012), activating frequent filter  
188 cleaning and reducing the residence time of reactant on the filter. The unstable HCl flow rate  
189 at the outlet of the 1<sup>st</sup> stage can in turn disturb the operation of the 2<sup>nd</sup> stage of acid gas  
190 removal.

191 In general, this control does not include the minimisation of reactant feed as a criterion and  
192 does not realise a rational use of reactant.

193

## 194 3 Methodology

### 195 3.1 Framework

196 Fig. 3 summarises the methodology developed to analyse the performance of alternative  
197 process control strategies for DSI, aimed at environmental and economic optimisation. The  
198 core element of the methodology is the development of a process simulation that allows  
199 exploring alternative control settings in a virtual console, while reducing the need for full-  
200 scale test-runs at the real plant. The process simulation duplicates into a software  
201 environment the process units and the control system of the actual facility. As sketched in Fig.  
202 3, building the simulation required: i) to reproduce the HCl removal process with a process  
203 model; and ii) to simulate the control structure of the DSI unit. The first task required the  
204 identification of an appropriate mathematical model for the description of the reaction  
205 process (see section 3.2) and its training and validation on plant data collected from test-runs



206 (see section 3.3). The second task was performed replicating the control architecture of the  
207 plant, briefly outlined in section 2.2, with a Simulink block diagram (see section 3.4).

208 The reliability of the simulation is validated considering the operating process control set-up  
209 in the real plant and comparing the outputs of the simulation with those recorded in the plant  
210 during normal operation, using the actual data as the input for the simulation. Once validated,  
211 the simulation can be used to screen and tune alternative control strategies, eventually  
212 leading to a new tuned control strategy that may be tested in the real plant, as in the test  
213 case that will be introduced in section 4.

214 Besides conventional indicators of process control performance, specific environmental and  
215 economic indicators (section 3.5) were defined to allow a comprehensive assessment of the  
216 performance of the alternative control strategies.

217

### 218 **3.2 Selection of data-driven process model and input variables**

219 As mentioned above, a mathematical model is required to reproduce the process dynamics  
220 in the simulation. The process model needs to predict how the instantaneous HCl removal  
221 efficiency varies depending on the inlet HCl concentration and the feed of solid reactant.  
222 Given the intrinsic unsteady nature of the process, this task can be addressed only with a  
223 dynamic model capable of handling the rapidly changing operating conditions (e.g. variability  
224 of HCl concentration due to variability of waste composition). Existing simplified stationary  
225 models of acid gas removal that are typically applied for process optimisation studies  
226 (Harriott, 1990; Dal Pozzo et al., 2016) are clearly not apt for this task. On the other hand,  
227 phenomenological models (Antonioni et al., 2016; Foo et al., 2017; Montagnaro et al., 2016)  
228 that describe rigorously the kinetic and mass transfer phenomena involved in the gas-solid  
229 reaction process were typically derived from laboratory-scale data and are not suitable to

230 simulate full-scale systems, as stated by Gutiérrez Ortiz and Ollero (2008) and Gassner et al.  
231 (2014).

232 Therefore, a data-driven approach was chosen. A system identification procedure was  
233 performed to estimate the structure and the parameters of the model from observed input-  
234 output plant data (Ljung, 2010). A simple input-output polynomial model, *i.e.* the linear auto-  
235 regressive exogenous (ARX) model, was selected as base for the system identification. ARX  
236 models have already demonstrated to be reliable tools in emission control problems, e.g. in  
237 the prediction of NO<sub>x</sub> (Smrekar et al., 2013) or SO<sub>x</sub> (Choi et al., 2002) emissions from coal-  
238 fired boilers. They are appreciated for their transparency and ease of interpretation (Akinola  
239 et al., 2019). The general form of an ARX model is the following:

240

$$241 \quad y(t) = a_1 y(t-1) + \dots + a_{n_a} y(t-n_a) + \sum_i [b_{1,i} u_i(t-n_k) + \dots + b_{n_b,i} u_i(t-n_{k,i}-n_{b,i}+1)] + e(t) \quad (4)$$

242

243 where  $y$  is the output variable,  $u_i$  are the  $i$  input variables considered in the model, and  $e$  is  
244 the white-noise disturbance value. The values  $a$  and  $b$  are the model parameters, which can  
245 be represented in compact form in the parameter vector  $\theta$ :

246

$$247 \quad \theta = [a_1 \dots a_{n_a} \ b_{1,i} \dots b_{n_b,i}]' \quad (5)$$

248

249 This model structure implies that the output variable  $y$  at time  $t$  is predicted as a linear  
250 combination of past output values (autoregressive part of the model) and current and past  
251 values of the input variables (exogenous part of the model). The parameters  $n_a$  and  $n_{b,i}$  are,  
252 respectively, the number of past output samples and the number of past input samples (for  
253 each input variable  $i$ ) considered for the prediction of the current output. The model can also

254 consider input delay terms  $n_{k,i}$ , i.e. the number of input samples that occur before the input  
255 affects the output (also known as the dead time of the system). The use of past observations  
256 in the prediction of the output allows approximating also derivative terms by difference  
257 quotients, thus enabling the reproduction of the dynamics of the modelled system. The  
258 numbers  $n_a$ ,  $n_{b,i}$  and  $n_{k,i}$  are known as hyperparameters and represent the order of the model,  
259 i.e. they indicate the number of parameters to optimise in the training of the model.

260 For the sake of simplicity, a two-input single-output ARX model was chosen for the present  
261 study. The modelled output  $y$  is the HCl molar flowrate in the flue gas leaving the DSI system.  
262 The two input variables  $u_i$  are the inlet HCl molar flowrate and the molar flowrate of  $\text{Ca}(\text{OH})_2$   
263 fed to the DSI system.

264 In general, other variables might also affect the HCl removal process. The second most  
265 abundant acid compound in WtE flue gases,  $\text{SO}_2$ , can consume a fraction of the reactant feed  
266 (Zhang et al., 2019). Fluctuations in the flue gas flowrate can influence reactant residence  
267 time (Hunt and Sewell, 2015). Variations in the operating temperature of the HCl removal  
268 stage, e.g. caused by fouling in the heat recovery section upstream, can alter the gas-solid  
269 reaction kinetics (Dal Pozzo et al., 2018c). However, variations of temperature and flue gas  
270 flowrate are typically limited (see Fig. 2d and 2e) and, in the WtE plant under study, the inlet  
271  $\text{SO}_2$  concentration was a couple of orders of magnitude lower than that of HCl. Therefore,  
272 these variables were excluded in the formulation of the model.

273

### 274 **3.3 Calibration of the model**

275 As a data-driven model, the ARX structure requires a specific calibration on data from the  
276 actual DSI system modelled. Informative data can be obtained by open-loop tests, in which

277 the control of the system is deactivated and process performance is assessed by varying  
278 manually the feed rate of reactant while recording inlet and outlet HCl concentration.

279 The dataset  $Z^N$ , formed by N consecutive observations of the input and output variables,  
280 obtained from the tests has to be divided in: i) a training set  $Z_{trn}$ , used for the estimation of  
281 the optimal model parameters; and, ii) a cross-validation set  $Z_{crv}$ , used for the selection of the  
282 optimal order of the model.

283 A further validation data set,  $Z_{val}$ , obtained collecting operating data from the normal, closed-  
284 loop operation of the DSI system can be used for the assessment of the performance of the  
285 trained model.

286 Denoting as  $\hat{y}(t|\theta)$  the output prediction of the model, least-square method is used to  
287 estimate the parameter vector  $\theta^*$  that produces the best fit of the training data  $Z_{trn}$ :

$$288 \theta^* = \arg \min\{V(\theta, Z_{trn})\}, \quad \text{where } V(\theta, Z_{trn}) = \frac{1}{N_{trn}} \sum_{t=0}^{N_{trn}-1} (y(t) - \hat{y}(t|\theta))^2 \quad (6)$$

289 The cross-validation compares the performance of models with different orders, each with its  
290 optimal parameter vector  $\theta_i^*$ , estimated from the training set. The best model is the one for  
291 which  $V(\theta, Z_{crv})$  is the smallest. This procedure helps selecting a model structure without  
292 unnecessary complexity (*i.e.* order), as excessively complex models tend to overfit the training  
293 set and perform poorly in the cross-validation set. Lastly, the model with order and  
294 parameters optimised for the  $Z_{trn}$  and  $Z_{crv}$  sets can be tested on the validation set  $Z_{val}$  and the  
295 procedure can go on iteratively until a given threshold of performance is fulfilled.

296

### 297 **3.4 Virtual console**

298 The process model described in section 3.2 was integrated into a simulation environment,  
299 where also the control loop and the other components of the DSI system were cloned as in

300 the real plant. The virtual console simulating the operation of the real DSI system consists of  
301 four blocks, as shown in Figure 4.

302 The block “*Data import*” defines the inlet conditions of the simulation (inlet HCl concentration  
303 and flue gas flowrate). These may be either actual plant data, collected at the measurement  
304 point PM1 (see Fig. 1), or artificial data, created to test the system performance under specific  
305 strain.

306 The input data of the “*Data Import*” block are then transferred to the “*DTS*” and “*DCS*” blocks.  
307 The “*DTS*” block contains the process model described in section 3.2. The “*DCS*” block  
308 simulates the control system described in section 2.2. Specifically, given as input signals the  
309 HCl load at the inlet of the DTS (provided by the “*Data Import*” block) and the HCl load at the  
310 outlet of the dry treatment system (modelled by the “*DTS*” block), this block evaluates with a  
311 clock time of 1 s the command input for the actuator that regulates the feed rate of Ca(OH)<sub>2</sub>.

312 The “*Actuator*” block simulates the operation of the screw feeder installed in the real plant.  
313 The virtual actuator receives a percentage command of rotational speed calculated by the  
314 “*DCS*” block and transforms it into a molar feed rate of solid reactant to the “*DTS*” block,  
315 following a linear relationship between percentage command and feed rate that is  
316 characteristic of the real feeder. The response of the actuator was modelled as a first order  
317 transfer function:

318

$$319 \quad G(s) = \frac{R}{T_m \cdot s + 1} \quad (7)$$

320

321 where  $T_m$  is the actuation time of the screw feeder and  $R$  is the command to feed rate ratio.

322 This console allows the comparative testing of the behaviour of the DSI system under the  
323 default control (section 2.2) or an alternative control, as discussed in the test case described  
324 in section 4.

325

### 326 **3.5 Performance indicators selected to test alternative control strategies**

327 Both conventional indicators for process control performance and specific indicators  
328 capturing the environmental and economic performance of the process were defined to allow  
329 a comparison of alternative control strategies. The indicators are reported in Table 1  
330 alongside their values obtained for the test case that will be introduced in section 4.

331 With respect to conventional process control indicators, these address the stability of the  
332 output variables. The *instability of reactant injection*, expressed as the ratio of the CV of  
333 reactant injection to the CV of inlet HCl mass flow, measures the time variability of the feed  
334 rate of reactant imposed by the control system. All things equal, a control demanding less  
335 variable feed rates is preferred as it induces less mechanical stress on the feeding system. The  
336 *instability of HCl outlet*, expressed as the ratio of the CV of outlet HCl mass flow to the CV of  
337 inlet HCl mass flow, measures the variability of the HCl mass flow at the outlet of the DSI  
338 system.

339 Environmental indicators trace the material streams responsible for the indirect  
340 environmental burdens of HCl removal: the *specific consumption of reactant*, expressed as  
341 mass of reactant injected per mass of removed HCl, and the *specific generation of residues*,  
342 expressed as mass of process residues generated per mass of removed HCl. These indicators  
343 were monitored both for the Ca-based 1<sup>st</sup> stage and the bicarbonate-fed 2<sup>nd</sup> stage of HCl  
344 removal, as the stabilisation of control in the 1<sup>st</sup> stage (object of the study) can also result in  
345 a more stable operation for the 2<sup>nd</sup> stage. Therefore, an indicator of *overall generation of*

346 *residues*, encompassing both treatment stages, was also considered to have a complete  
347 picture of the environmental benefit of control optimisation.

348 Lastly, an indicator addressing *overall operating costs* was also estimated, by translating the  
349 streams of reactants and residues in operating costs considering their unit costs (see Table  
350 S1).

351

## 352 **4 Test Case**

353

### 354 **4.1 Definition of the test case**

355 The test facility described in section 2.1 was used to define a test case for the application of  
356 the methodology outlined in section 3. An open-loop test-run was used for the calibration of  
357 the ARX model, while the accuracy of the resulting virtual console in reproducing the system  
358 behaviour under its default control was assessed using several datasets available for the  
359 normal operation of the DSI system. An example of alternative control was proposed, tuned  
360 in the virtual console, then tested by full-scale test-runs on the real plant. The set of indicators  
361 defined in section 3.4 was adopted to quantify the improvements in the stability of process  
362 control and the economic and environmental performance.

363

### 364 **4.2 Calibration of the model and validation of the simulation for the test case**

365 The behaviour of the DSI system of the test facility was studied via step-response tests (Liu  
366 and Gao, 2012). Input excitations were applied to the system by varying stepwise the feed  
367 rate of  $\text{Ca}(\text{OH})_2$ . The effect on system behaviour was recorded by continuous monitoring (**30**  
368 **s resolution time**) of the outlet HCl concentration (measurement point PM2 in Fig. 1), while  
369 the inlet HCl concentration was also recorded (measurement point PM1 in Fig. 1).

370 On the basis of the discussion provided in section 3.2, the ARX model was calibrated  
371 considering the molar flowrate of inlet HCl (calculated from the measured inlet HCl  
372 concentration and inlet flue gas flowrate) and the feed rate of Ca(OH)<sub>2</sub> as input variables,  
373 while the molar flowrate of outlet HCl (product of the measured outlet HCl concentration  
374 and outlet flue gas flowrate) is the modelled output.

375 The virtual console including the calibrated process model was then validated, comparing its  
376 simulated outlet of HCl with the measured values in four datasets of operation of the DSI  
377 system under the reference control, provided the same input data (see section 5.1). The  
378 simulation error was quantitatively assessed by calculating a cumulative normalised root  
379 mean squared error (RMSE):

$$380 \text{ Normalised RMSE } (t) = \frac{\sqrt{\frac{1}{n(t)} \sum_{i=1}^{n(t)} (y_i - \hat{y}_i)^2}}{\frac{\sum_{i=1}^{n(t)} y_i}{n(t)}} \quad (8)$$

381 where  $n(t)$  is the number of measurements/model evaluations at a given time.

382

### 383 4.3 Selection and tuning of an alternative control

384 Once the accuracy of the simulation results was demonstrated, the virtual console was used  
385 to test alternative approaches to the control of HCl removal operation. In this test case, the  
386 control logic described in section 2.2 (named in the following as “conventional control”) was  
387 substituted with a simple feedback control (named in the following as “alternative control”).  
388 Recalling Fig. 2, the conventional control is built to suppress any overrun of the setpoint of  
389 outlet HCl concentration with a spike of Ca(OH)<sub>2</sub> feed. The consequences of such approach,  
390 as illustrated in section 2.3, are an excess consumption of Ca(OH)<sub>2</sub> and unstable inlet  
391 conditions for the 2<sup>nd</sup> HCl removal stage fed with NaHCO<sub>3</sub>, which, again, lead typically to an



392 excess consumption of  $\text{NaHCO}_3$ . Conversely, a properly tuned control in purely feedback  
393 action could limit the variability of both reactant feed and outlet HCl concentration.

394 The proposed feedback control is a simple proportional integral (PI) control. As the HCl inlet  
395 concentration signal is by nature highly variable and vulnerable to noise contamination  
396 (Coleman et al., 2019), the introduction of a derivative (D) control term was avoided, as it  
397 could generate system instability (Ting et al., 2008).

398 Hence, in the simulation the two parameters of the feedback control,  $K_p$  gain and  $\tau_I$  integral  
399 time, were tuned. The values of the optimised parameters were  $K_p = 2$  and  $\tau_I = 345$  s.

400

#### 401 **4.4 Performance assessment of the new control at the real plant**

402 Eventually, a comparative assessment of the performance of the conventional and alternative  
403 control was carried out at the test facility. The alternative control was easily implemented, by  
404 deactivating the feedforward control and updating the feedback settings to the tuned  
405 parameters.

406 The test consisted in comparing a period of DSI process operation with the alternative control  
407 with a period of operation with the conventional control. The HCl load released by waste  
408 combustion can vary widely over time, and any control logic would manage better a low and  
409 uniform inlet mass flow of HCl, rather than a high and fluctuating one. Thus, to ensure a  
410 proper comparison, a period of operation experiencing an almost equal inlet mass flow of HCl  
411 to that present during the test of the alternative control was selected as representative of the  
412 conventional control performance.

413 **As a measure of variability of inlet HCl load, the coefficient of variation (CV) of the HCl mass**  
414 **flow during the test period was estimated:**

415

416  $CV = \frac{\sigma}{\mu}$  (9)

417

418 where  $\sigma$  and  $\mu$  are respectively the standard deviation and the mean of the measurements of  
419 inlet HCl mass flow during the period of study. It was also ensured that the two periods of DSI  
420 operation used for the comparison exhibited a similar CV of HCl mass flow, as it will be  
421 discussed in section 5.3. The HCl removal efficiency  $X$  was also calculated as follows:

422  $X = \frac{\dot{m}_{HCl,in} - \dot{m}_{HCl,out}}{\dot{m}_{HCl,in}}$  (10)

423 The comparison among the performance of the alternative control strategies was carried out  
424 calculating the indicators discussed in section 3.5.

425

## 426 5 Results and Discussion

### 427 5.1 Results of the validation of the simulation

428 Figure 5 reports the performance of the virtual console in simulating the behaviour of the  
429 conventional process control of the DSI system on a sample dataset (other samples are shown  
430 in Figures S1-S3 in the Supporting Information, SI). The percentage command to reactant feed  
431 given by the real system and by the simulation are compared in Fig. 5a. Figure 5b compares  
432 the measured and the simulated outlet HCl mass flow. The yellow curve represents the set  
433 value of outlet HCl mass flow, which is a fluctuating value as it is defined as the product of the  
434 fixed setpoint of outlet HCl concentration (see e.g. Fig. 2b) and the variable value of the flue  
435 gas flowrate (see e.g. Fig. 2d). Again, it can be noticed that the conventional control treats the  
436 set value more like a threshold than a setpoint, as discussed in section 2.3. Figure 5c plots the  
437 cumulative average error of the simulation, represented as a normalised RMSE (introduced  
438 in section 4.2). The error increases over time, indicating a loss of performance of the process

439 model nested in the simulation, that is typical of error accumulation in models of  
440 autoregressive nature (Bazghaleh et al., 2013; Nelles, 2020). As evidenced also by the figures  
441 in the SI, the error grows faster when outlet HCl fluctuates widely, while it remains almost  
442 unchanged and may even decrease during periods of stable operation. It is clear that a simple  
443 ARX model, linear by nature, falls short of achieving an accurate instantaneous prediction of  
444 HCl outlet, which is the result of a complex and non-linear process involving gas-solid  
445 reactions both in duct and on filter bags. Nonetheless, the simulation captures the average  
446 system behaviour with acceptable resolution for the objective of the study.

447

## 448 **5.2 Results of the virtual testing of the alternative control**

449 The simulation was used for the tuning and for the virtual testing of the alternative PI control.  
450 The tuning of the alternative control by the methodology outlined in section 4.3 provided the  
451 following value for the control parameters: proportional gain  $K_p = 2$  and integral time  $\tau_I$  of  
452 345 s. It should be recalled that the PI settings of the feedback component of the conventional  
453 control (see section 2.2) are  $K_p = 5$  and  $\tau_I = 8$  s. The alternative control is less aggressive,  
454 with a reduced proportional action and a significantly higher integral time, which lowers the  
455 sensitivity of the control action to temporary deviations of the inlet HCl load. Figure 6a  
456 illustrates the different behaviour of the alternative control strategy compared to the  
457 conventional process control, on a data sample of 100 min. The simulation of the alternative  
458 control was started during a significant deviation of the measured HCl outlet concentration  
459 from the set-point value to emphasise the different mode of operation of the two control  
460 strategies. The feed rate variations imposed by the alternative control strategy are markedly  
461 smoother than those of the conventional control. The proposed strategy accepts momentary  
462 upticks in the HCl outlet concentration, whereas the action of the original control results in

463 spikes of reactant feed. Conversely, the alternative control strategy imposes a slightly higher  
464 feed rate than the original control during periods in which the latter operates in the  
465 feedforward mode. These opposite behaviours are evident from the plot of cumulated  
466 reactant consumption reported in Fig. 6c. Given that the variability of the reactant feed rate  
467 has been highlighted in section 2.3 as one of the main causes of inefficient reactant  
468 exploitation in the DTS, the alternative control strategy appears well suited to rationalise the  
469 use of the reactant, thus minimising the resulting generation of process residues.

470

### 471 **5.3 Results of the field test of the alternative control**

472 The alternative PI control was implemented in the DCS of the test facility. As outlined in  
473 section 4.4, a test run of the new control was carried out and the resulting operational data  
474 were compared with a previous period under the conventional process control configuration.  
475 The equivalence of action between the two controls was guaranteed by selecting the average  
476 value of outlet HCl concentration in the previous day under the conventional control as the  
477 setpoint for the test of the alternative control (see Fig. 7b).

478 Two 5-hour data samples with similar inlet flue gas conditions were selected for the  
479 comparative assessment. The two time series are shown in Fig. 7a, where it is possible to  
480 compare qualitatively the behaviour of the two control strategies, i.e. the feed rate of  
481 reactant and the outlet HCl flowrate, depending on the inlet HCl flowrate. The relative  
482 performance of the two controls was tracked via the indicators introduced in section 3.5.  
483 Table 1 provides the list of the indicators used and the specific values obtained, while Figure  
484 7c shows a radar plot comparing the normalised values of the performance indicators of the  
485 alternative control to the reference one. Internal normalisation was used to obtain the values  
486 shown in the figure. Given the low inlet SO<sub>2</sub> concentrations measured at the plant (in the

487 range 10 – 30 mg/Nm<sup>3</sup>) and the relatively low reactivity compared to HCl, the effect of SO<sub>2</sub> on  
488 system performance is negligible and not discussed in the analysis.

489 First of all, the two 5-hour data samples present highly comparable inlet HCl loads, hence the  
490 two controls are tested in a situation of similar stress. As reported in Table 1, the average inlet  
491 HCl mass flow rate in the two periods is equal and its CV is 68% higher during the test of the  
492 alternative control, i.e. the selection of data samples is slightly biased in favour of the  
493 conventional control.

494 Figure 7 shows that the real behaviour of the proposed PI-only control is in line with what was  
495 expected from the virtual simulation (see Fig. 6). The feed rate varies smoothly, with slow  
496 corrections in face of any sharp variation in the outlet HCl flow. Conversely, the conventional  
497 control reacts aggressively to deviations in the HCl outlet, with the characteristic spikes of  
498 reactant feed rate already described in Fig. 2.

499 When the performance indicators introduced in section 3.5 are considered, the parameter  
500 instability of reactant injection captures numerically this difference: while the commanded  
501 feed rate of the original control shows a CV that is 4.3 times higher than the CV of the inlet  
502 HCl molar flow, the CV of the commanded feed rate of the proposed control is only 1.24 times  
503 higher (a 71% reduction, see Table 1).

504 At the same time, the specific consumption of reactant in the Ca(OH)<sub>2</sub>-fed treatment stage is  
505 11% lower with the proposed control. This confirms that the lower aggressivity of the new  
506 control settings is not detrimental to the HCl removal efficiency of the system. On the  
507 contrary, in the test period, the proposed control managed to achieve the desired HCl  
508 removal performance with a significantly lower variability of reactant feed rate, which has the  
509 further advantage of reducing the mechanical stress to the screw feeder and the reactant  
510 transport system.

511 Another relevant metric is the instability of the outlet HCl flow, defined in section 3.5 as the  
512 ratio between the CVs of outlet and inlet HCl molar flow. The proposed PI-only control  
513 achieves a 39% reduction in this indicator. This means that the HCl load exiting the  $\text{Ca(OH)}_2$ -  
514 fed treatment stage is less variable in time, thus the downstream  $\text{NaHCO}_3$ -fed stage operates  
515 on a less variable HCl inlet and is put in less stressful working conditions. As a consequence,  
516 the optimisation of the control in the  $\text{Ca(OH)}_2$  stage generates also a 26% reduction in the  
517 specific consumption of reactant in the subsequent  $\text{NaHCO}_3$  stage (see again Table 1), whose  
518 control was not modified.

519 The overall consequence of the increase in efficiency owing to the new PI-only control is the  
520 reduction in the production of the solid process residues of HCl removal via both the gas-solid  
521 reactions with  $\text{Ca(OH)}_2$  and  $\text{NaHCO}_3$ . The new control achieves a 7% and a 22% reduction in  
522 the generation of process residues, respectively in the 1<sup>st</sup> and 2<sup>nd</sup> treatment stages. The  
523 overall effect is a 13% reduction of the amount of process waste generated by the HCl removal  
524 operation. A further confirmation of this effect can be observed in figure S4 in the SI, which  
525 shows the simulated action of the conventional control system considering the inlet HCl load  
526 for the 5-hour dataset collected during the test-run. The figure evidences that the multiple  
527 activations of the feedback mode would have caused a higher reactant consumption.

528

#### 529 **5.4 Discussion**

530 In the light of the indicators in Table 1, the alternative control strategy tuned in the virtual  
531 simulation was demonstrated to improve the overall economic and environmental  
532 performance of the system. The consumption of reactants and the generation of process  
533 residues were lowered in both the treatment stages, by increasing the efficiency of reactant  
534 delivery. It was thus demonstrated that the main drawback of dry acid gas removal, i.e. the

535 required high excess of reactant, can be partially mitigated by introducing specific process  
536 control strategies. In particular, for a multistage system as that of the test facility, it is worth  
537 highlighting that an intervention limited to the 1<sup>st</sup> treatment stage can produce benefits also  
538 on the 2<sup>nd</sup> stage, by enabling a more efficient operation thanks to the lowered variability of  
539 the inlet HCl.

540 The alternative control strategy, based on a PI feedback control, however, has clear  
541 limitations: even if the simple feedback action reduces the variability of HCl load compared  
542 to the conventional control, the instability with respect to a setpoint is still quite high. More  
543 advanced control strategies could offer further improvements. Nonetheless, the proposed  
544 solution achieved the results in Table 1 with minimal need of full-scale testing and no  
545 significant change in the control architecture of the system, demonstrating the ease of  
546 implementation of better solid waste and reactant management via control optimisation.

547 The results obtained show that the procedure developed for the test of alternative control  
548 strategies, based on a virtual console, and the metric introduced, based on the performance  
549 indicators listed in Table 1, provide an effective approach to allow the improvement of the  
550 environmental and economic operational performance of acid gas treatment systems.

551

## 552 6 Conclusions

553 With increasingly strict limits on the emission of airborne pollutants as HCl, the flue gas  
554 treatment sections in WtE installations are experiencing problems of excessive consumption  
555 of reactants and related high generation of solid residues destined to landfilling, which lead  
556 to non-negligible indirect environmental burdens. By considering a reference state-of-the-art  
557 acid gas removal system, the present study demonstrated that a standard process control

558 approach based exclusively on the suppression of HCl emissions might be a suboptimal  
559 solution in terms of economic and environmental performance. A simple methodology based  
560 on virtual simulation and limited full-scale test-runs allowed identifying and tuning an  
561 alternative control strategy that achieved a reduction in the generation of solid process  
562 residues equal to 7% in the optimised  $\text{Ca}(\text{OH})_2$ -fed 1<sup>st</sup> stage of HCl removal and 13% in the  
563 overall two-stage treatment line with respect to the original control configuration, while  
564 maintaining the same HCl emission performance at stack.

565 Despite the relevant advantages in terms of reactant economy, a limitation of the proposed  
566 solution is that it only partially alleviates the fluctuations in the HCl concentration at the outlet  
567 of the 1<sup>st</sup> treatment stage, which are intrinsic to the WtE context. More advanced process  
568 control strategies, taking into account process disturbances other than inlet pollutant  
569 concentration and reactant feed rate, could be the key to develop plant-specific highly  
570 performant model-based control schemes. However, the present study evidenced that  
571 process control optimisation is a promising area of improvement in the management of WtE  
572 flue gas treatment, not only to improve stable operation, but also to increase significantly the  
573 economic and environmental performance of DSI processes without hindering the  
574 compliance to emission limits at stack.

575



576 **References**

- 577 Akinola, T.E., Oko, E., Gu, Y., Wei, H.-L., Wang, M., 2019. Non-linear system identification  
578 of solvent-based post-combustion CO<sub>2</sub> capture process. *Fuel* 239, 1213-1223.
- 579 Antonioni, G., Dal Pozzo, A., Guglielmi, D., Tugnoli, A., Cozzani, V., 2016. Enhanced  
580 modelling of heterogeneous gas-solid reactions in acid gas removal dry processes. *Chem.*  
581 *Eng. Sci.* 148, 140-154.
- 582 Ardolino, F., Boccia, C., Arena, U., 2020. Environmental performances of a modern waste-  
583 to-energy unit in the light of the 2019 BREF document. *Waste Manage.* 104, 94-103.
- 584 Arena, U., 2015. From waste-to-energy to waste-to-resources: The new role of thermal  
585 treatments of solid waste in the Recycling Society. *Waste Manage.* 37, 1-2.
- 586 Bagheri, M., Esfilar, R., Golchi, M.S., Kennedy, C.A., 2020. Towards a circular economy: A  
587 comprehensive study of higher heat values and emission potential of various municipal  
588 solid wastes. *Waste Manage.* 101, 210-221.
- 589 Bal, M., Reddy, T.T., Meikap, B.C., 2019. Removal of HCl gas from off gases using self-  
590 priming venturi scrubber. *J. Haz. Mat.* 364, 406-418.
- 591 **Bazghaleh, M., Mohammadzaheri, M., Grainger, S., Cazzolato, B., Lu, T.-F., 2013. A new**  
592 **hybrid method for sensorless control of piezoelectric actuators. *Sensors and Actuators A:***  
593 ***Physical* 194, 25-30.**
- 594 Beylot, A., Hochar, A., Michel, P., Descat, M., Ménard, Y., Villeneuve, J., 2018. Municipal  
595 Solid Waste Incineration in France: An Overview of Air Pollution Control Techniques,  
596 Emissions, and Energy Efficiency. *J. Ind. Ecol.* 22, 1016-1026.
- 597 Bogush, A., Stegemann, J.A., Wood, I., Roy, A., 2015. Element composition and  
598 mineralogical characterisation of air pollution control residue from UK energy-from-waste  
599 facilities. *Waste Manage.* 36, 119-129.
- 600 **CEN, 2019. CEN/TS 17337:2019 – Stationary source emissions - Determination of mass**  
601 **concentration of multiple gaseous species - Fourier transform infrared spectroscopy.**  
602 **European Committee for Standardization, Bruxelles, Belgium.**
- 603 Choi, S., Yoo, C., Lee, I.-B., 2002. SO<sub>x</sub> monitoring and neural net classification in the power  
604 plant. *J. Environ. Eng.* 128, 911-918.
- 605 Cignitti, S., Mansouri, S.S., Sales-Cruz, M., Jensen, F., Huusom, J.K., 2016. Dynamic  
606 Modeling and Analysis of an Industrial Gas Suspension Absorber for Flue Gas  
607 Desulfurization. *Emiss. Control Sci. Technol.* 2, 20-32.
- 608 Coleman, M.D., Ellison, M., Robinson, R.A., Gardiner, T.D., Smith, T.O.M., 2019.  
609 Uncertainty requirements of the European Union's Industrial Emissions Directive for  
610 monitoring sulfur dioxide emissions: Implications from a blind comparison of sulfate  
611 measurements by accredited laboratories. *J. Air Waste Manage. Assoc.* 69, 1070-1078.
- 612 Dal Pozzo, A., Moricone, R., Tugnoli, A., Cozzani, V., 2019. Experimental Investigation of  
613 the Reactivity of Sodium Bicarbonate toward Hydrogen Chloride and Sulfur Dioxide at Low  
614 Temperatures. *Ind. Eng. Chem. Res.* 58, 6316-6324.

615 Dal Pozzo, A., Lazazzara, L., Antonioni, G., Cozzani, V., 2020. Techno-economic  
616 performance of HCl and SO<sub>2</sub> removal in waste-to-energy plants by furnace direct sorbent  
617 injection. *J. Haz. Mat.* 394, 122518.

618 Dal Pozzo, A., Guglielmi, D., Antonioni, G., Tugnoli, A., 2018a. Environmental and  
619 economic performance assessment of alternative acid gas removal technologies for  
620 waste-to-energy plants. *Sust. Prod. Consumption* 16, 202-215.

621 Dal Pozzo, A., Armutlulu, A., Rekhtina, M., Müller, C.R., Cozzani, V. 2018b. CO<sub>2</sub> Uptake  
622 Potential of Ca-Based Air Pollution Control Residues over Repeated Carbonation-  
623 Calcination Cycles. *Energy Fuels* 32, 5386-5395.

624 Dal Pozzo, A., Giannella, M., Antonioni, G., Cozzani, V., 2018c. Optimization of the  
625 economic and environmental profile of HCl removal in a municipal solid waste incinerator  
626 through historical data analysis. *Chem. Eng. Trans.* 67, 463-468.

627 Dal Pozzo, A., Guglielmi, D., Antonioni, G., Tugnoli, A., 2017. Sustainability analysis of dry  
628 treatment technologies for acid gas removal in waste-to-energy plants. *J. Clean. Prod.* 162,  
629 1061-1074.

630 Dal Pozzo, A., Antonioni, G., Guglielmi, D., Stramigioli, C., Cozzani, V., 2016. Comparison  
631 of alternative flue gas dry treatment technologies in waste-to-energy processes. *Waste  
632 Manage.* 51, 81-90.

633 Damgaard, A., Riber, C., Fruergaard, T., Hulgaard, T., Christensen, T.H., 2010. Life-cycle-  
634 assessment of the historical development of air pollution control and energy recovery in  
635 waste incineration. *Waste Manage.* 30, 1244-1250.

636 De Greef, J., Villani, K., Goethals, J., Van Belle, H., Van Caneghem, J., Vandecasteele, C.,  
637 2013. Optimising energy recovery and use of chemicals, resources and materials in  
638 modern waste-to-energy plants. *Waste Manage.* 33, 2416-2424.

639 Dong, J., Jeswani, H.K., Nzihou, A., Azapagic, A., 2020. The environmental cost of  
640 recovering energy from municipal solid waste. *Appl. Energy* 267, 114792.

641 Ephraim, A., Ngo, L.D., Pham Minh, D., Lebonnois, D., Peregrina, C., Sharrock, P., Nzihou,  
642 A., 2019. Valorization of Waste-Derived Inorganic Sorbents for the Removal of HCl in  
643 Syngas. *Waste Biomass Valorization* 10, 3435-3446.

644 Foo, R., Berger, R., Heiszwolf, J.J., 2016. Reaction Kinetic Modeling of DSI for MATS  
645 Compliance. In: Proceedings of the Power Plant Pollutant Control and Carbon  
646 Management "MEGA" Symposium, Baltimore, MD, USA, 16–19 August 2016

647 Gassner, M., Nilsson, J., Nilsson, E., Palmé, T., Züfle, H., Bernero, S., 2014. A data-driven  
648 approach for analysing the operational behaviour and performance of an industrial flue  
649 gas desulphurisation process. *Computer Aided Chem. Eng.* 33, 661-666.

650 Gerassimidou, S., Velis, C.A., Williams, P.T., Castaldi, M.J., Black, L., Komilis, D., 2020.  
651 Chlorine in waste-derived solid recovered fuel (SRF), co-combusted in cement kilns: A  
652 systematic review of sources, reactions, fate and implications. *Critical Reviews in  
653 Environmental Science and Technology*, in press.

654 Goodall, P.; Sharpe, R.; West, A., 2019. A data-driven simulation to support  
655 remanufacturing operations. *Computers in Industry* 105, 48-60.

656 Guo, Y., Xu, Z., Zheng, C., Shu, J., Dong, H., Zhang, Y., Weng, W., Gao, X., 2019. Modeling  
657 and optimization of wet flue gas desulfurization system based on a hybrid modeling  
658 method. *J. Air Waste Manage. Assoc.* 69, 565-575.

659 Gutiérrez Ortiz, F.J., Ollero, P., 2008. A realistic approach to modeling an in-duct  
660 desulfurization process based on an experimental pilot plant study. *Chem. Eng. J.* 141,  
661 141-150.

662 Harriott, P., 1990. A Simple Model for SO<sub>2</sub> Removal in the Duct Injection Process. *J. Air  
663 Waste Manage. Assoc.* 40, 998-1003.

664 **Hartman, M., Svoboda, K., Pohorely, M., Syc, M., 2013. Thermal Decomposition of Sodium  
665 Hydrogen Carbonate and Textural Features of Its Calcines. *Ind. Eng. Chem. Res.* 52, 10619-  
666 10626.**

667 **Hunt, G., Sewell, M., 2015. Utilizing Dry Sorbent Injection Technology to Improve Acid Gas  
668 Control. In: 34th International Conference on Thermal Treatment Technologies &  
669 Hazardous Waste Combustors, Houston, TX, USA, 20-22 October 2015**

670 Iizuka, A., Morishita, Y., Shibata, E., Takatoh, C., Cho, H., 2020. Basic Study of the Reaction  
671 of Calcium Hydroxide with Hydrogen Chloride Using Single Crystals. *Ind. Eng. Chem. Res.*  
672 59, 9699-9704.

673 Kameda, T., Tochinai, M., Kumagai, S., Yoshioka, T., 2020. Treatment of HCl gas by cyclic  
674 use of Mg–Al layered double hydroxide intercalated with CO<sub>3</sub><sup>2-</sup>. *Atmospheric Pollution  
675 Res.* 11, 290-295.

676 Kim, K.-D., Jeon, S.-M., Hasolli, N., Lee, K.-S., Lee, J.-R., Han, J.-W., Kim, H.T., Park, Y.-O.,  
677 2017. HCl removal characteristics of calcium hydroxide at the dry-type sorbent reaction  
678 accelerator using municipal waste incinerator flue gas at a real site. *Korean J Chem Eng*  
679 34, 747-756.

680 Kockmann, N., 2019. Digital methods and tools for chemical equipment and plants. *Reaction  
681 Chemistry and Engineering* 4, 1522-1529.

682 Lausset, C., Cherubini, F., del Alamo Serrano, G., Becidan, M., Strømman, A.H., 2016.  
683 Life-cycle assessment of a Waste-to-Energy plant in central Norway: Current situation and  
684 effects of changes in waste fraction composition. *Waste Manage.* 58, 191-201.

685 Liu, T., Gao, F., 2012. Step Response Identification of Stable Processes. In: Liu, T., Gao, F.,  
686 *Industrial Process Identification and Control Design*, Springer-Verlag London, London, UK.

687 Liu, S., Sun, L., Zhu, S., (...), Chen, X., Zhong, W., 2020. Operation strategy optimization of  
688 desulfurization system based on data mining. *Appl. Mathematical Modelling* 81, 144-158.

689 Ljung, L., 2010. Perspectives on system identification. *Annual Reviews in Control* 34, 1-12.

690 Margallo, M., Taddei, M.B.M., Hernández-Pellón, A., Aldaco, R., Irabien, A., 2015.  
691 Environmental sustainability assessment of the management of municipal solid waste  
692 incineration residues: A review of the current situation. *Clean Technol. Environ. Policy* 17,  
693 1333-1353.

694 Montagnaro, F., Balsamo, M., Salatino, P., 2016. A single particle model of lime sulphation  
695 with a fractal formulation of product layer diffusion. *Chem. Eng. Sci.* 156, 115-120.

696 Muratori, G., Dal Pozzo, A., Antonioni, G., Cozzani, V., 2020. Application of Multivariate  
697 Statistical Methods to the Modelling of a Flue Gas Treatment Stage in a Waste-to-energy  
698 Plant. *Chem. Eng. Trans.* 82, 397-402.

699 Nelles, O., 2020. *Nonlinear System Identification: From Classical Approaches to Neural*  
700 *Networks, Fuzzy Models, and Gaussian Processes.* Springer Nature, Berlin, Germany.

701 Neuwahl, F., Cusano, G., Gomez Benavides, J., Holbrook, S., Roudier, S., 2019. Best  
702 Available Techniques (BAT) Reference Document for Waste Incineration. EUR 29971 EN.  
703 doi:10.2760/761437

704 Ouda, O.K.M., Raza, S.A., Nizami, A.S., Rehan, M., Al-Waked, R., Korres, N.E., 2016. Waste  
705 to energy potential: A case study of Saudi Arabia. *Renewable Sustainable Energy Reviews*  
706 61, 328-340.

707 Peng, H., Ozaki, T., Toyoda, Y., Shioya, H., Nakano, K., Haggan-Ozaki, V., Mori, M., 2004.  
708 RBF-ARX model-based nonlinear system modeling and predictive control with application  
709 to a NO<sub>x</sub> decomposition process. *Control Engineering Practice* 12, 191-203.

710 Quina, M.J., Bontempi, E., Bogush, A., Schlumberger, S., Weibel, G., Braga, R., Funari, V.,  
711 Hyks, J., Rasmussen, E., Lederer, J., 2018. Technologies for the management of MSW  
712 incineration ashes from gas cleaning: New perspectives on recovery of secondary raw  
713 materials and circular economy. *Sci. Total Environ.* 635, 526-542.

714 Saleem, M., Krammer, G., 2012. On the Stability of Pulse-Jet Regenerated-Bag Filter  
715 Operation. *Chemical Engineering and Technology* 35, 877-884.

716 Smrekar, J., Potočnik, P., Senegačnik, A., 2013. Multi-step-ahead prediction of NO<sub>x</sub>  
717 emissions for a coal-based boiler. *Appl. Energy* 106, 89-99.

718 Ting, C.-H., Chen, H.-H., Yen, C.-C., 2008. A PID ratio control for removal of HCl/SO<sub>x</sub> in flue  
719 gas from refuse municipal incinerators. *Control Engineering Practice* 16, 286-293.

720 Van Caneghem, J., Van Acker, K., De Greef, J., Wauters, G., Vandecasteele, C., 2019.  
721 Waste-to-energy is compatible and complementary with recycling in the circular  
722 economy. *Clean Technol. Environ. Policy*, in press.

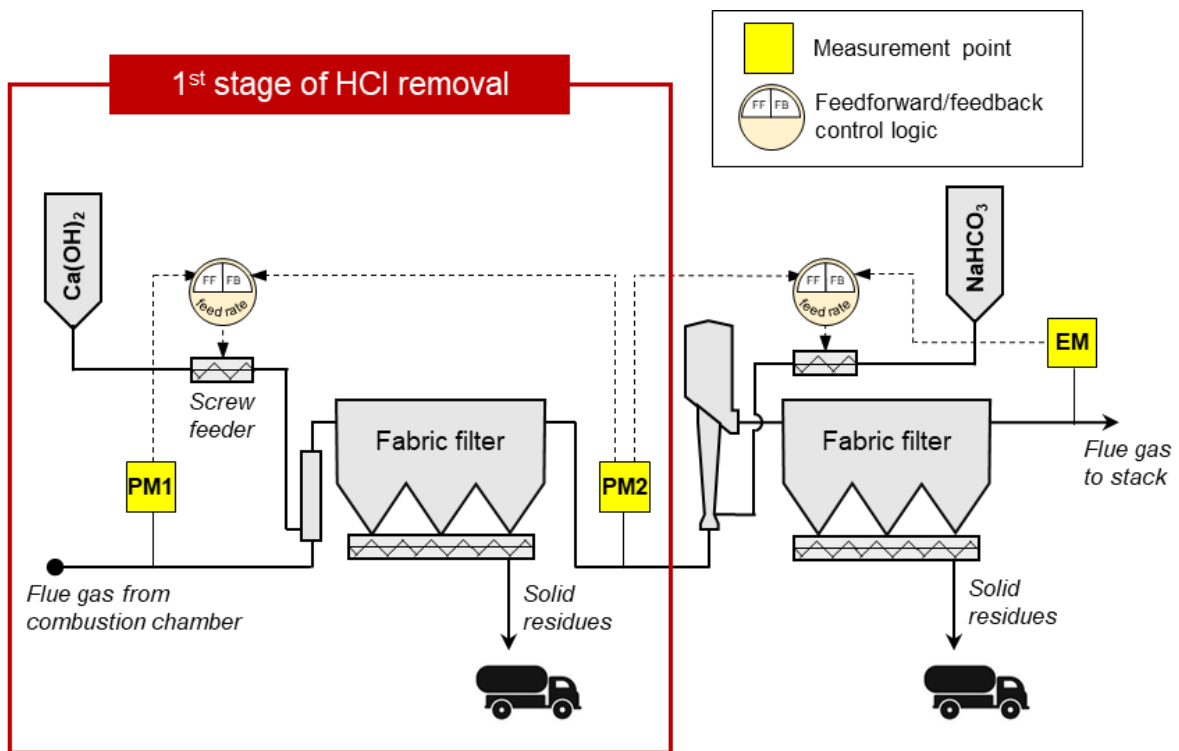
723 Vehlow, J., 2015. Air pollution control systems in WtE units: An overview. *Waste Manage.*  
724 37, 58-74.

725 Wu, C., Kang, S.-J., Keener, T.C., Lee, S.-K., 2004. A model for dry sodium bicarbonate duct  
726 injection flue gas desulfurization. *Advances in Environmental Research* 8, 655-666.

727 Yang, N., Damgaard, A., Scheutz, C., Shao, L.-M., He, P.-J., 2018. A comparison of chemical  
728 MSW compositional data between China and Denmark. *J. Environ. Sci.* 74, 1-10.

729 Zhang, H., Yu, S., Shao, L., He, P., 2019. Estimating source strengths of HCl and SO<sub>2</sub>  
730 emissions in the flue gas from waste incineration. *J. Environ. Sci.* 75, 370-377.

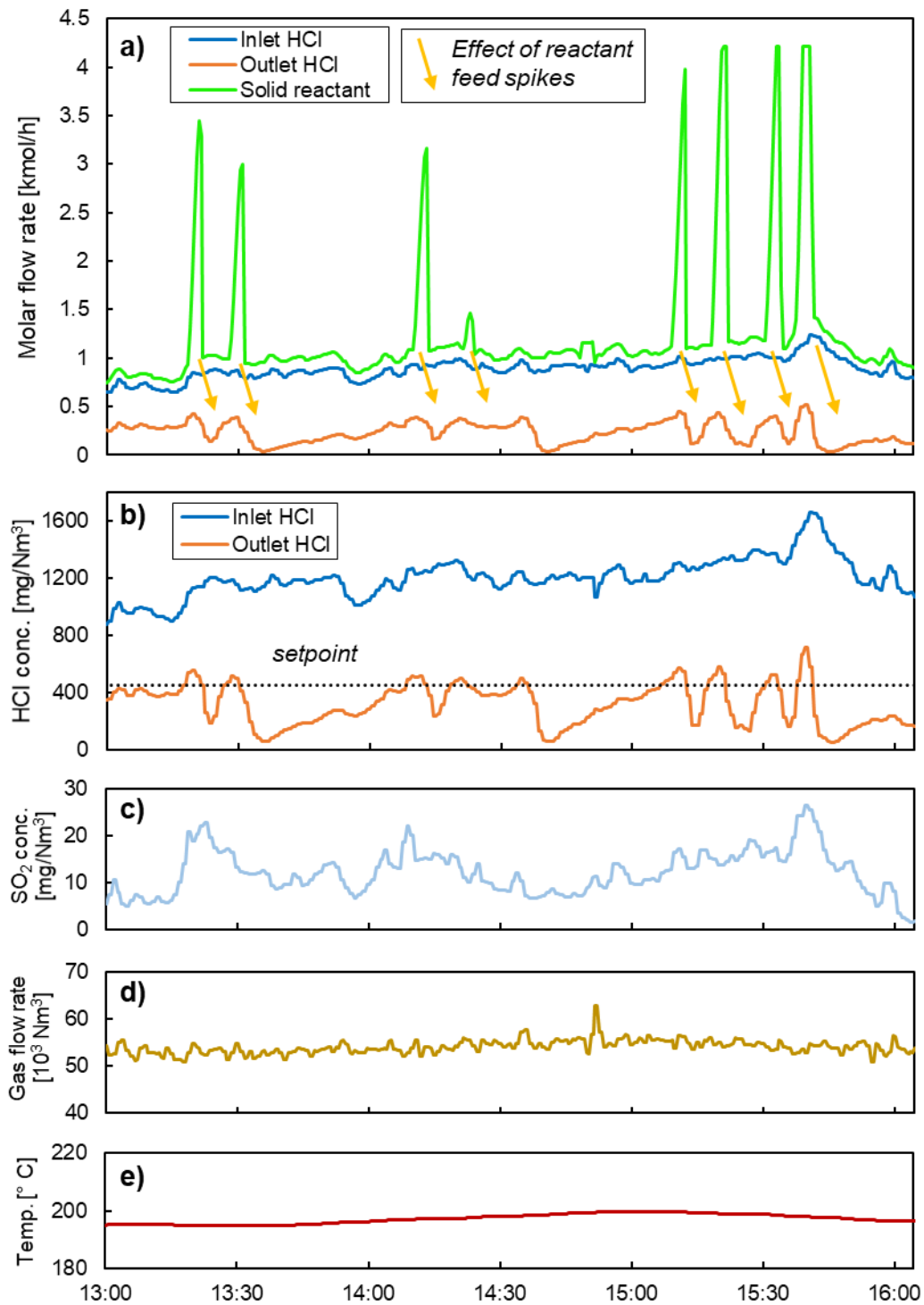
731  
732  
733  
734  
735



738

739 **Figure 1.** Scheme of the two-stage acid gas abatement system of the test facility considered,  
 740 including measurement points of flue gas composition (PM1, PM2 = process measurement,  
 741 EM = measurement at stack) and control loops for reactant feed rate. Control optimization of  
 742 1<sup>st</sup> stage (red box in the figure) was the object of the study.

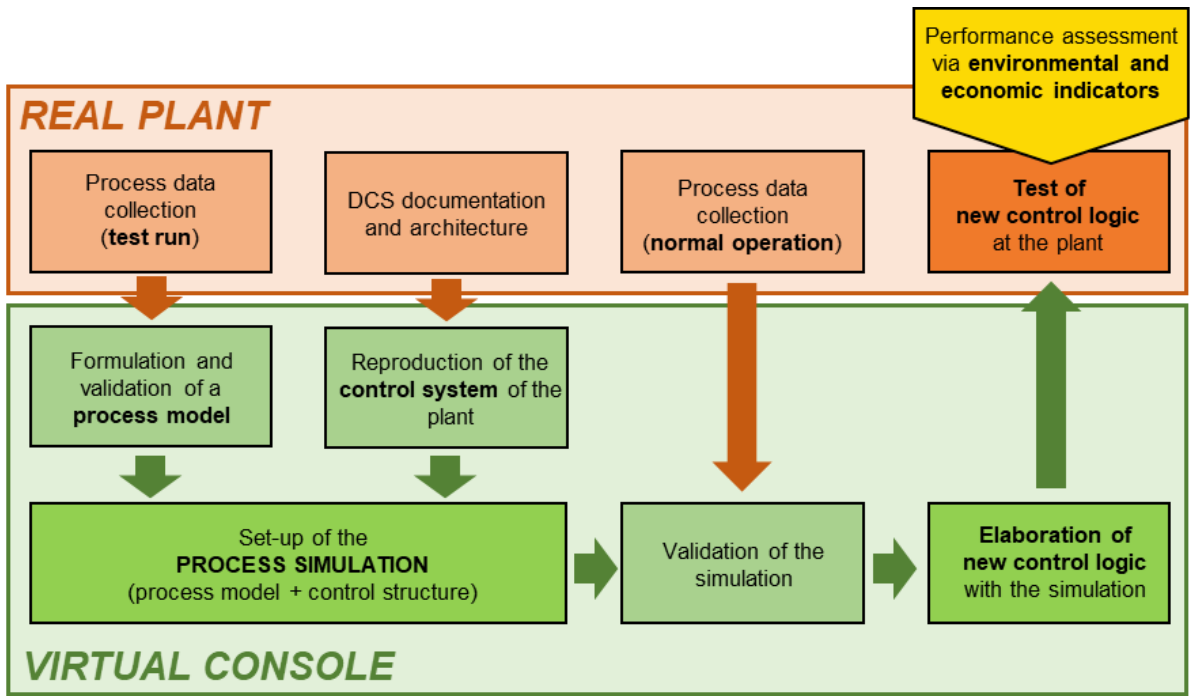
743



744

745 **Figure 2.** Data recorded by the distributed control system (DCS) of an Italian WtE facility  
 746 showing: a) the typical trend of inlet and outlet HCl flowrate and solid reactant feed rate  
 747 during normal operation of the 1<sup>st</sup> stage acid gas removal unit applying the conventional  
 748 process control strategy; b) threshold setpoint with respect to HCl inlet and outlet  
 749 concentrations; c) SO<sub>2</sub> concentration; d) flue gas flowrate; e) operating temperature.

750



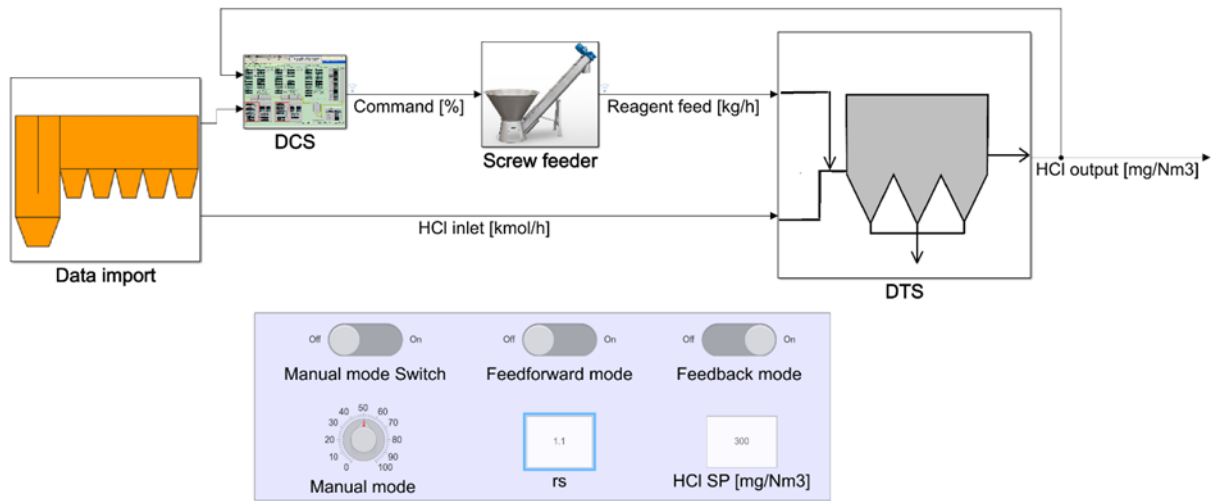
751

752 **Figure 3.** Methodology developed for testing and tuning of improved process control

753 strategies.

754

755



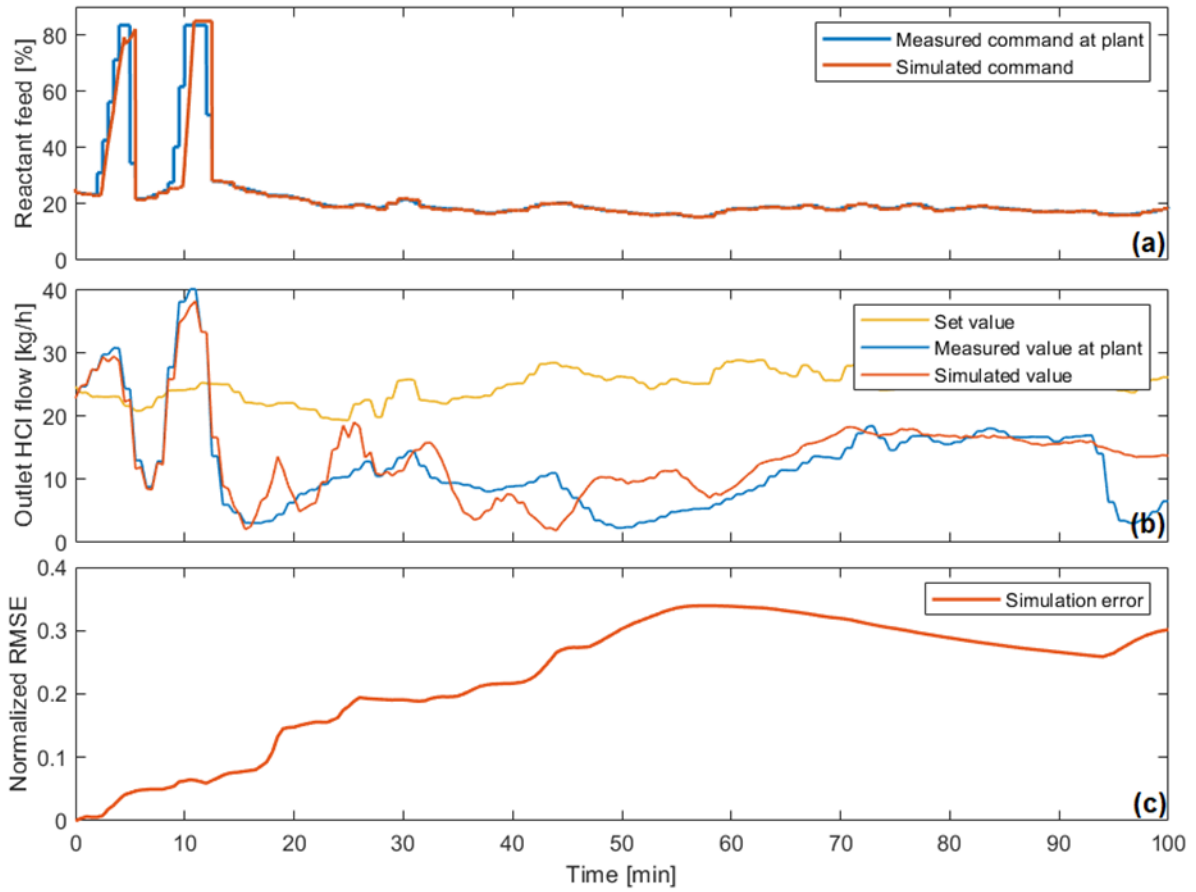
756

757 **Figure 4.** Virtual console developed to simulate the DSI process (1<sup>st</sup> stage of the acid gas

758 removal system in Fig. 1) using the Simulink<sup>®</sup> software tool.

759

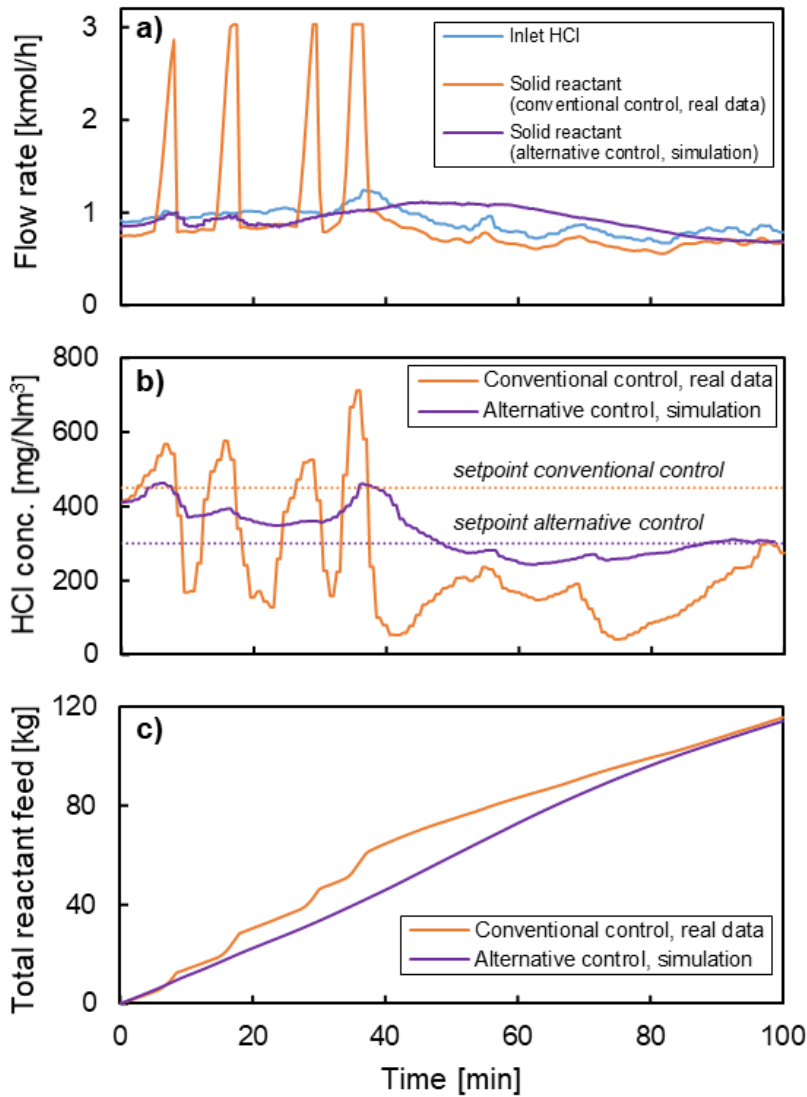




760  
761

762 **Figure 5.** Performance of the virtual console in simulating the behaviour of the conventional  
 763 control of the system: a) measured vs. simulated command of reactant feed, b) measured vs.  
 764 simulated outlet HCl flow rate, compared to the set value of the control, c) cumulative average  
 765 error of the simulation.

766



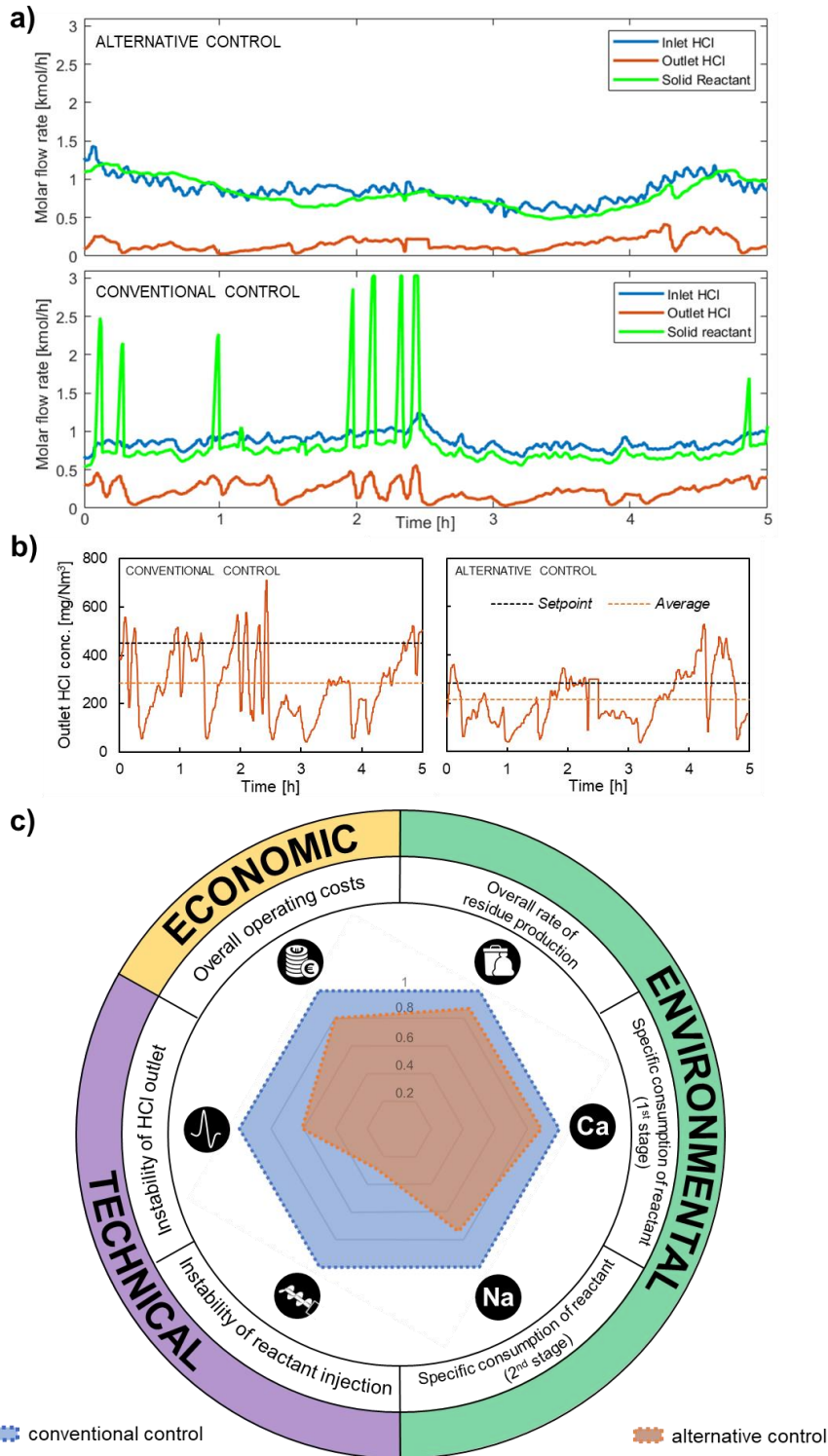
767

768 **Figure 6.** a) Simulation of the reactant feed rate by the alternative PI control strategy

769 compared to the conventional process control on a sample dataset; b) deviation of the outlet

770 HCl concentration from the respective setpoints, c) resulting cumulated reactant consumption.

771



772

773 **Figure 7.** Results of test-run: a) 5-hour data samples obtained during alternative process  
 774 control and conventional process control operation under a similar HCl input, b) outlet HCl  
 775 concentration in the two 5-hour data samples, c) comparison between the normalised  
 776 performance indicators of the alternative process control strategy to the conventional process  
 777 control.

778 **Table 1.** Performance of the alternative control strategy vs. the conventional process control  
 779 monitored according to the performance indicators introduced in section 3.5.

Parameter or indicator		Test period		$\Delta$
		Conventional control	Alternative control	
Inlet HCl mass flow rate (kg/h)	$\mu$	64.4	64.4	-
	CV	0.12	0.19	+68%
Feed rate of reactant, Ca(OH) <sub>2</sub> (kg/h)	$\mu$	61.1	60.0	-2%
	CV	0.49	0.24	-52%
Outlet HCl mass flow rate (kg/h)	$\mu$	17.2	12.5	-27%
	CV	0.51	0.52	+2%
HCl removal efficiency (%)	$\mu$	75.8	82.3	+9%
	CV	11.2	8.5	-24%
<b>Instability of reactant injection</b> (CV of Ca(OH) <sub>2</sub> feed rate / CV of inlet HCl)		4.27	1.24	<b>-71%</b>
<b>Instability of HCl outlet</b> (CV of outlet HCl / CV of inlet HCl)		4.4	2.7	<b>-39%</b>
<b>Specific consumption of reactant</b> (1 <sup>st</sup> stage) (kg of Ca(OH) <sub>2</sub> fed / kg of HCl removed)		1.30	1.16	<b>-11%</b>
<b>Specific generation of residues</b> (1 <sup>st</sup> stage) (kg of residues / kg of HCl removed)		1.80	1.67	<b>-7%</b>
<b>Specific consumption of reactant</b> (2 <sup>nd</sup> stage) (kg of NaHCO <sub>3</sub> fed / kg of HCl removed)		3.85	2.86	<b>-26%</b>
<b>Specific generation of residues</b> (2 <sup>nd</sup> stage) (kg of residues / kg of HCl removed)		2.55	2.00	<b>-22%</b>
<b>Overall rate of residue production</b> (kg of residues / kg of HCl removed)		2.00	1.73	<b>-13%</b>
<b>Overall economic performance</b> (€ of operating costs / kg of HCl removed)		1.86	1.48	<b>-20%</b>

780

781

**Declaration of interests**

The authors declare that they have no known competing financial interests or personal relationships that could have appeared to influence the work reported in this paper.

The authors declare the following financial interests/personal relationships which may be considered as potential competing interests:



Click here to access/download

**Supplementary Material**

Suppl Info WM\_Control\_revFINAL.docx

